HARVARD UNIVERSITY

THE GRADUATE SCHOOL OF ARTS AND SCIENCES

THESIS ACCEPTANCE CERTIFICATE

(To be placed in Original Copy)

The undersigned, appointed by the

Division

Department Organismic and Evolutionary Biology

Committee

have examined a thesis entitled

Two Mechanisms for the Initiation of Embolism in Tracheary Elements and Other Dead Plant Cells Under Water Stress.

presented by

Ann Marie Lewis

candidate for the degree of Doctor of Philosophy and hereby certify that it is worthy of acceptance.

Signature .....

Typed name John G. Torrey

Signature .....

Typed name Melvin T. Tyree

Signature .....

Typed name P. B. Tomlinson

Date July 16, 1987

Two Mechanisms for the Initiation of Embolism in Tracheary Elements and Other Dead Plant Cells Under Water Stress

A thesis presented

by

Ann Marie Lewis

to

The Department of Organismic and Evolutionary Biology

in partial fulfillment of the requirements

for the degree of

Doctor of Philosophy

in the subject of

Biology

Harvard University

Cambridge, Massachusetts

July 1987

ABSTRACT

Two of the mechanisms that have been proposed to explain embolism in plants under water stress are shown to cause emboli in dead plant cells. The first is "air-seeding" (i.e., the nucleation of a gas embolus by the entry of an external air bubble through a hole in the cell wall), and the second is nucleation by a bubble trapped in the cell lumen. Both in *Sphagnum* hyalocysts and in *Thuja occidentalis* L. tracheids, emboli develop by air-seeding when no bubbles are entrapped at the onset of dehydration. Cells which contain bubbles develop emboli by expansion of the trapped bubbles. Furthermore, experiments show that the pressure differential at which a cell air-seeds is predicted by the capillary equation and is dependent upon the diameter of the hyaline pores in *Sphagnum* and on the diameter of the pores in the pit membranes of *T. occidentalis*. Direct proof that ultrasonic acoustic emissions and emboli occur simultaneously in dehydrating tissue gives further evidence that the production of ultrasonic emissions is a good indicator of cavitations. Cavitations can be caused by air-seeding and can lead to the development of emboli. The research uses anatomical techniques, traditional and modified physiological methods, and advanced pressure probe and ultrasonic technology. This combination is used for the first time to give direct evidence for some previously elusive answers to questions in water transport and storage in plants.

CONTENTS IN BRIEF

TABLE OF CONTENTS

ACKNOWLEDGMENTS

The late Dr. Martin H. Zimmermann introduced me to the mysteries of water transport in plants; without his contagious excitement and initial guidance, this project would not have been possible. Dr. Melvin T. Tyree took on the responsibility of guiding this project from afar. I am grateful to him, not only for his advice, monetary support, and ferry service to Snake Island, but also to him and his family for their hospitality and friendship. Drs. J.G. Torrey and P.B. Tomlinson gave me advice and support at my home institution. I am especially grateful to P.B.T. for finally surrendering in the battle to turn me into an anatomist! Dr. C. Tubbs of the USDA-Forest Service persevered to provide funding and equipment. M.R. Mattmuller gave technical assistance and provided levity at the critical times. J.M. Sipe assisted with the tedious counting and measuring of tracheids. Dr. J.S. Sperry helped in more ways than he can imagine. Dr. D.J. Cosgrove and the members of his laboratory provided equipment and moral support during pressure microprobing. I cannot enumerate the ways in which the secretarial staff, woods crew, faculty, and visitors (from such places as Canada, China, France, Israel, Japan, New Zealand, Poland, and W. Germany) at the Harvard Forest, Petersham MA helped to provide a pleasant working and living environment. Special thanks are due to E.R. Boose., especially for his help in presenting the equivalent pore diameter material.

Major funding came from the Minority Prize Fellowship and the Department of OEB at Harvard University, and from a Cooperative Education Agreement between the USDA-Forest Service and Harvard

University. The Maria Moors Cabot Foundation, at the Harvard Forest, and the Harvard Forest provided additional funding and facilities.

Dedicated

to

my parents Willesse and Strickland Lewis, for the trips to the science museums, for the patient schooling, and for exposure to a broad world; to my other parents, Evelyn and Emery Boose, for their confidence and encouragement; but this thesis is especially dedicated to the folks who dream and to those who need to dream. May they be so fortunate as to have the desire, the opportunity, and the support in the requisite combination to help themselves and others attain their goals, for it is all too easy for many people to take education and achievement for granted.

CHAPTER 1

Introduction: Embolism Processes in Plant Cells

In every vascular plant examined in recent studies, dead xylem elements develop gas bubbles when the plant is exposed to severe enough water stress (for examples, see Bailey, 1916; Crombie et al., 1985b; Sperry, 1985; Tyree and Dixon, 1986; Zimmermann, 1983, and literature cited therein; cf., Dixon, 1924, pp. 11 to 13). The generally accepted sequence of events which leads to bubble development is as follows: 1) Water stress develops by evaporation of water from the plant body more quickly than water can be absorbed; plant water potential (Ψ [psi]) decreases. 2) As Ψ decreases, the lumen water potential of xylem sap-filled tracheary elements decreases, due almost entirely to lowering of the pressure potential (Ψ_p). 3) Gas bubbles form in the lumens. Generally, the gas formation is considered to be a sudden and energetic event, and the term "cavitation" is used to describe the phenomenon (Oertli, 1971; Pickard, 1981; Tyree and Dixon, 1983). Only one cavitation is required to disrupt the integrity of the sap in a conduit (i.e., tracheid, fiber, or vessel). 4) Negative Ψ_p causes a basic instability which forces the bubble to expand, fill the conduit, and block water transport. 5) The original gas bubble, thought to be primarily water vapor, becomes infiltrated with air by diffusion from intercellular spaces and from the exterior. The air bubble effectively prevents the conduit from transporting xylem sap even at a slightly

higher Ψ. The air blockage is known as an air embolism. Until recently, little was known of the events which occur at the cellular level to initiate the collapse of a water column in a conduit.

Much of the terminology of xylem transport is borrowed from the fields of medicine and physics where the systems studied function at pressures above vacuum. Xylem transport frequently occurs under conditions of extreme (high) tension, i.e., negative pressure ($\Psi_p \leq -0.1$ MPa [megapascals] or pressures below 0 MPa absolute). Researchers in plant water transport are currently defining and refining terminology as understanding of the processes improves. In this text these terms will be used as follows:

Cavitation--the sudden and energetic breakage of a water column in an enclosed space, such as a tracheid lumen. The breakage may be caused by the spontaneous failure of intermolecular bonds within the water itself or by the introduction of a gas, liquid, or solid discontinuity (i.e., nucleus) which seeds the breakdown of intermolecular water bonds. This definition differs from that presented by Apfel (1972) who limits cavitation to events that occur in the absence of an interface.

Embolus--any gas bubble within the lumen of a tracheary element that significantly lowers the conduction of xylem sap through that element at the applied Ψ_p, or pressure gradient. An air embolus is a bubble composed of a gaseous mixture containing nitrogen, oxygen, and carbon dioxide in close to the same proportions that they are found in air. Even at pressures

above 0.1 MPa, an air bubble may continue to exist and effectively block transport through a conduit. At a given temperature and pressure, an air bubble may either remain stable, dissolve, or expand depending on its radius (see Ewers, 1985; Sperry, 1986, Ward et al., 1982); thus an air bubble may be an embolus at one pressure and not at another. It is important to note that water vapor may form cavities large enough to significantly decrease the conductance of a conduit when $\Psi_p \leq 0$ MPa. Bubbles composed exclusively of water vapor collapse instantly at pressures above 0.0023 MPa (the vapor pressure of water at 20^{o}C); thus, vapor blocks at pressures below vacuum are not blocks at pressures much above vacuum. In the past, water vapor bubbles were not usually referred to as emboli, but it is convenient to have an all inclusive term pertaining to any bubble which disrupts sap flow. When it is important to distinguish between types, they may be referred to as air emboli or (water) vapor emboli. In general, an air bubble is an effective embolus over a wider range of Ψ_p than a vapor bubble.

Embolism--the blockage of significant xylem sap transport through a tracheary element effected by an embolus. Blocks caused by air emboli and by vapor emboli may be referred to as air embolism and vapor embolism, respectively.

General acceptance of these, or similar, definitions in plant water relations would help to simplify descriptions of xylem processes and lessen the confusion resulting from terms that are not clearly defined

with respect to plants.

How does the initial air or water vapor cavity form? Several hypotheses have been discussed in the literature. Oertli (1971) and Pickard (1981) have presented overviews; Pickard's is the more comprehensive. As discussed by these two authors, several processes have threshold pressures that, in theory, are far below any pressures measured in plants. Two such processes, i.e., the formation of a gas filled cavity by random dissolved gas molecules being released from solution to create a bubble, and the spontaneous rarification of water molecules to form a water vapor cavity in place of liquid water, theoretically require xylem pressure potentials on the order of -100 to -1000 MPa before such events are likely to effect the system detectably. On the other hand, the lowest pressures measured in plants are in the range of -30 to -40 MPa in the annulus cells of fern sporangia at sporangial dehiscence (Renner, 1915). More commonly, Ψ, and thus xylem Ψ_p, ranges from 0 to -8 MPa in vascular plants (Scholander et al., 1965). Attempts have been made to determine the validity of the theoretical values for cavitation by the spontaneous breakdown of intermolecular bonds in water and by dissolved gases coming out of solution. It has not been possible to cause cavitation by one of these means at ambient temperature because the tension required is unattainable. Some estimates are extrapolated from related experiments at high temperature and atmospheric pressure (cf. Apfel, 1972). The estimates agree well with theoretical values. It is very unlikely that cavitation in plants occurs by one of these mechanisms.

There are three processes which may function within the pressure range that has been measured in plants (Fig. 1.1). They are

1) "air-seeding," 2) nucleation at an entrapped bubble, and 3) nucleation at a hydrophobic surface. In air-seeding, the pressure differential across an air-water meniscus in a pore or crack in a cell wall forces the meniscus through the pore into the cell lumen. This process creates a bubble in the lumen of the cell which then expands to create an embolus. The behavior of the meniscus in the pore should be described by the capillary equation, since the pore can be thought of as a very short capillary tube. When a pre-existing bubble expands to become the embolus in a cell, the original entrapped bubble can either be free-floating in the cell sap or caught in a crack in the cell wall. Unless otherwise specified, the term "entrapped bubble" in the context of this thesis refers to a bubble contained in a cell lumen at the onset of dehydration which is free-floating (not attached to a wall or confined to a crack or other small depression in the cell wall). Nucleation at a hydrophobic surface does not require that a gas be present at the interface of a hydrophobic (wall) surface and water before tension builds. When the lumen pressure decreases, the repelling forces between the wall and the water force separation of the two at the site and water spontaneously evaporates into the developing void. The air-seeding and the entrapped bubble hypotheses are investigated in this thesis; the third hypothesis is not addressed in this research.

The three processes are not necessarily distinct. The point at which a free floating bubble becomes a bubble trapped in a wall crack, and the point at which a meniscus entering through a pore is distinguishable from a meniscus expanding from a crack is not clear (Fig. 1.2). Similarly, the distinction between a small air bubble

trapped in a crack and a few molecules of air trapped between water and a hydrophobic wall surface is subtle.

The research presented here tests for the occurrence of air-seeding and nucleation by an entrapped bubble in *Sphagnum* hyalocysts and in *Thuja occidentalis* tracheids. Traditional anatomical and physiological methods (e.g., histological staining and use of the pressure bomb) are modified and combined with more modern methods (e.g., ultrasonic detection as an indicator of cavitation and use of the pressure microprobe) in order to directly or more directly test hypotheses that the use of strictly conventional botanical techniques could not test.

The following chapters present the research and results in encapsulated units:

Chapter 2 proves the validity of using the capillary equation to describe the behavior of air-water menisci in plant cell pores by correlating lumen water potentials at bubble entry and pore diameters in *Sphagnum* hyalocysts. The behavior of bubbles which are trapped in the hyalocyst lumens at the onset of dehydration is reported. The possibility of using the hyalocyst as a model for tracheids and vessels during dehydration is presented.

Chapter 3 presents evidence that ultrasonic acoustic emissions are good indicators of cavitation in *Thuja occidentalis* tracheids.

Chapter 4 shows that air-seeding is a likely explanation for cavitation in *Thuja occidentalis* because the lumen water

potentials during air-seeding are predicted by the capillary equation given the pore diameters in the tracheid-to-tracheid pit membranes. The behavior of entrapped bubbles is described. The pattern of embolism within the xylem is related to our concept of embolism induced by water stress.

Chapter 5 discusses the overall significance of the results from the previous three chapters. In essence, both air-seeding and entrapped bubbles nucleate embolism in plants under water stress.

LITERATURE CITED

Apfel RE 1972 The tensile strength of liquids. Sci Amer 227: 58-71

Bailey IW 1916 The structure of the bordered pits of conifers and its bearing upon the tension hypothesis of the ascent of sap in plants. Bot Gaz 62: 133-142, 1 plate

Crombie DS, JA Milburn, MF Hipkins 1985b Maximum sustainable xylem sap tensions in *Rhododendron* and other species. Planta 163: 27-33

Dixon HH 1924 The Transpiration Stream. University of London Press, Ltd., London

Ewers F 1985 Xylem structure and water conduction in conifer trees, dicot trees, and lianas. IAWA Bull ns6: 309-317

Oertli JJ 1971 The stability of water under tension in the xylem. Z Pflanzenphysiol 65: S195-209

Pickard WF 1981 The ascent of sap in plants. Prog Biophys molec Biol 37: 181-229

Renner O 1915 Theoretisches und Experimentelles zür Kohäsionstheorie der Wasserbewegung. Jahr wiss Botanik 56: 617-667

Scholander PF, HT Hammel, ED Bradstreet, EA Hemmingsen 1965 Sap pressure in vascular plants: negative hydrostatic pressure can be measured in plants. Science 148: 339-346

Sperry JS 1985 Xylem embolism in the palm *Rhapis excelsa*. IAWA Bull ns6: 283-292

Sperry JS 1986 Relationship of xylem embolism to xylem pressure potential, stomatal closure, and shoot morphology in the palm *Rhapis excelsa*. Plant Physiol 80: 110-116

Tyree MT, MA Dixon 1983 Cavitation events in *Thuja occidentalis* L.?:

ultrasonic acoustic emissions from the sapwood can be measured. Plant Physiol 72: 1094-1099

Tyree MT, MA Dixon 1986 Water stress induced cavitation and embolism in some woody plants. Physiol Plant 66: 397-405

Ward CA, P Tikuisis, RD Venter 1982 Stability of bubbles in a closed volume of liquid-gas solution. J Appl Phys 53: 6076-6084

Weast RC, ed 1968 CRC Handbook of Chemistry and Physics. The Chemical Rubber Co., Cleveland OH

Zimmermann MH 1983 Xylem Structure and the Ascent of Sap. Springer-Verlag, Berlin, Heidelberg, New York, Tokyo

Fig. 1.1. Three mechanisms for the initiation of embolism. A, In air-seeding an air bubble pulls through a pore or crack in the cell wall when the lumen pressure is sufficiently below the external pressure. B, A bubble trapped in the cell lumen expands as the lumen pressure decreases. C, As the lumen pressure decreases, the repelling forces between water and a hydrophobic surface cause separation, and water evaporates into the void.

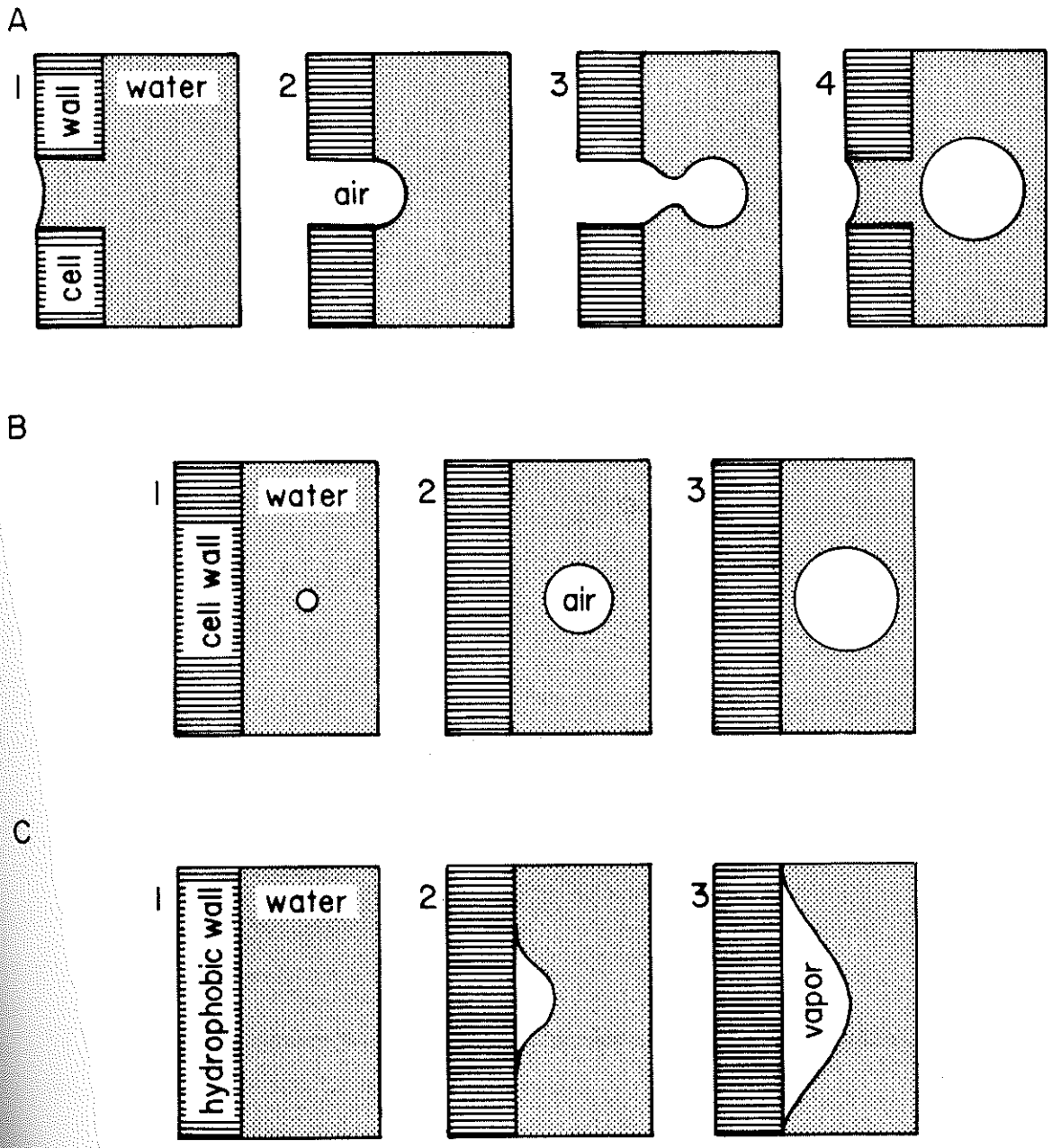
A
1
wall
water
cell
2
air
3
4
B
1
water
cell wall
2
air
3
C
1
hydrophobic wall
water
2
3
vapor

Fig. 1.2. Continuity among processes that initiate embolism. It may be difficult to distinguish between a free-floating bubble and a bubble that is trapped in a crack in the cell wall, as in A; between a bubble in contact with external air via a crack in the cell wall and an entrapped bubble which has no contact with external air, as in B; and between separation at a hydrophobic surface and expansion of a bubble trapped at a hydrophobic surface, as in C.

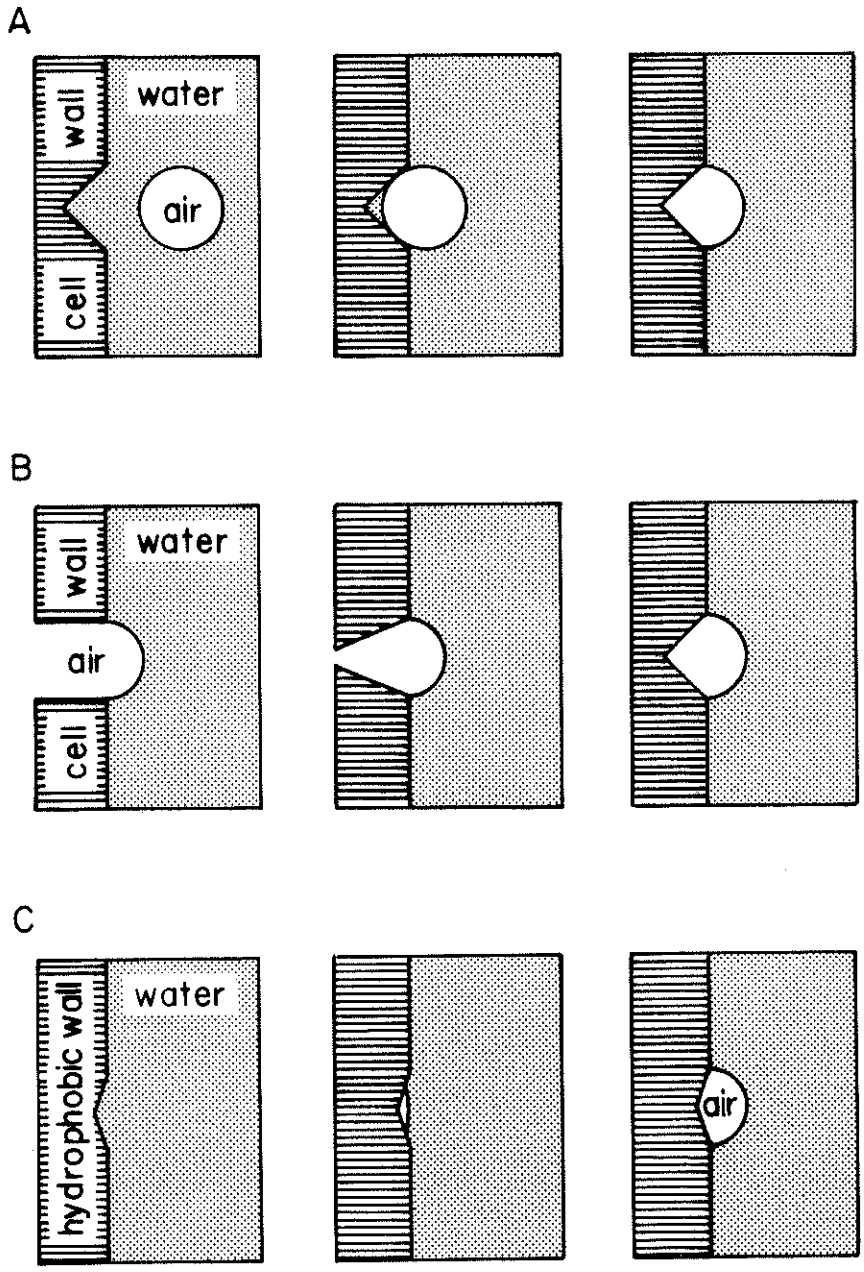
A
wall
water
air
cell
B
wall
water
air
cell
C
hydrophobic wall
water
air

CHAPTER 2

A Test of the Air-seeding Hypothesis Using *Sphagnum* Hyalocysts[1]

INTRODUCTION

In 1983, Zimmermann (1983) coined the term "air-seeding" to describe the hypothetical process in which an air bubble is pulled, under tension, into a lumen through a hole in the cell wall. At least since the early 1900's, botanists have discussed the possibility of cells embolizing by this method (Bailey, 1916; Clymo and Hayward, 1982; Crombie et al., 1985a; Huber,1956; Oertli, 1971; Pickard, 1981; Renner, 1925; Tyree and Dixon, 1986). Verification of air-seeding in cells has proved difficult because of the difficulty of confirming the initiation of a small bubble (frequently less than 1 μm) in a relatively large cell (usually more than 1 mm in length), while eliminating the possibility of embolism from other sources. Renner (1925) did conclude that pores in the outer wall of annulus cells on fern leptosporangia were approximately the right diameter (10 nm) to account for bubble entry through the walls at -30 MPa water potential as predicted by the capillary equation (Equation 1). By indirect methods, he measured cell water potentials in this range at spore discharge which is caused by sudden embolism of the annulus cells. Evidence of air-seeding in tracheary elements is presented by Sperry et al. (1987) who demonstrated that the pressure required to blow air through *Vitis* stems

---

[1] This chapter has been submitted Plant Physiology for publication.

agrees with that predicted by the capillary equation for pore diameters previously measured in temperate hardwood species. They also found that very low pressure air could not be blown through *Vitis* stems until the stems were dehydrated on the countertop to water potentials that corresponded to the applied pressure differentials at which higher pressure air could be blown through the stems. They did not correlate their results with water potentials at which cavitation could be detected by other means. Crombie et al. (1985a) demonstrated that the pressure required to blow air through hydrated *Rhododendron* stems is approximately that at which cavitation occurs in its leaves and shoots.

As part of a project to test more thoroughly the air-seeding hypothesis, an investigation into the mechanisms of embolism in *Sphagnum* was undertaken. *Sphagnum,* commonly known as peat moss, is a non-vascular plant of wet places. It is especially appropriate for studies on embolism because it has a network of dead water storage cells in its leaves. The leaves are one cell thick, and events during dehydration and rehydration can easily be seen in the water storage cells, the hyalocysts, under a light microscope. Generally, each hyalocyst has an empty lumen, spiral thickenings on the inner wall surface, and one or more pores aligned along the margins of the abaxial cell surface and occasionally along the margins of the adaxial cell surface (Fig. 2.1). The pores are perforations in the cell wall communicating between the external air and the empty lumen (Fig. 2.2). These pores probably contribute to the ability of *Sphagnum* to recover and to rapidly restore photosynthetic processes after having been dehydrated to brittleness. As a hyalocyst dehydrates, a bubble pulls through a pore, filling the lumen with air; water is released and flows

to the surrounding tissue. This paper presents the first direct measurements of lumen pressure at embolism, and by comparing the lumen pressures with pore diameters measured directly from the embolized cells, provides evidence that the lumen pressure measured when a bubble enters a hyalocyst agrees with that predicted by the capillary equation. Because the air-seeding hypothesis is based on the capillary equation, these experiments are the first direct test of the air-seeding hypothesis.

MATERIALS AND METHODS

The Capillary Equation and the Air-seeding Hypothesis. According to theory, when the meniscus first develops in a pore during air-seeding, the meniscus radius is very large, much larger than the radius of the pore. As the tension in the lumen increases during dehydration, the pressure difference across the meniscus increases, thus decreasing the meniscus radius to approach the pore radius. When the pressure differential reaches a critical value, the meniscus radius equals the pore radius, and the resultant bubble penetrates the pore and expands under tension to embolize the cell.

The pressure exerted by a column of water in a capillary tube is described by

$$P = \frac{2T\cos\Theta}{r} \qquad \text{Equation 1}$$

where T is the surface tension at the meniscus, Θ is the contact angle

between the water and the tube, and r is the internal radius of the tube. The equation can be thought of as describing the behavior of a meniscus in an elongated pore as a function of the pressures involved. Equation 1 is numerically

$$\Delta P \tilde{=} 0.3/D \qquad \text{Equation 2}$$

where ΔP is the pressure difference (MPa) across the meniscus, and D is the pore diameter (μm) (see the chapter's Appendix for a more complete discussion). A hyalocyst should embolize when the difference between ambient and lumen pressure is equal to that described by Equation 2 for the largest diameter pore in the cell.

Plant Material. Since the diameters of hyaline pores vary with species, several species of *Sphagnum* were collected at the Harvard Forest, Petersham MA. The reported measurements are for *S. compactum* DC., *S. girgensohnii* Russow, and *S. lindbergii* Lindb. Leaves were taken from branches in the apical tuft. The largest pore diameter in typical hyalocysts of tuft branch leaves ranged from 5 to 25 μm.

Observation of Embolism. Observation of embolism was facilitated by recording the dehydration and rehydration of hyalocysts on movie film at various speeds between 18 and 64 frames per second and on videotape at normal speed to allow repeated viewing of a particular sequence both at normal speed and in slow motion.

Lumen Pressure Measurements. Individual hyaline lumen tensions were measured using a pressure microprobe. The microprobe was developed originally to measure positive pressures in growing cells

(Hüsken et al., 1978). It was modified by Cosgrove (1985), who kindly assisted with further hardware and methodology alterations to permit measurements below atmospheric pressure. Nonami et al. (1987) give an interesting account of the positive pressure microprobe method. The probe is essentially an oil-filled glass capillary with one end in contact with a pressure transducer and mounted on a micromanipulator (Fig. 2.3). The other end is inserted into a hyalocyst through a pore. The probed, hydrated leaf is held securely on a glass slide, and viewed with a 50X long working-distance objective (working distance = 6 mm) on a compound microscope with a stationary stage (Bausch and Lomb MicroZoom Microscope). Total magnification was 750X. In order to permit dehydration by evaporation, the sample was not enclosed in a humidity chamber, as is usual for positive pressure measurements. A Leitz micromanipulator improved the maneuverability of the probe. The maximum angle of inclination below horizontal (15^{o}) of this manipulator was just sufficient to allow insertion of the probe through a hyaline pore of some hyalocysts without interference from the convex wall of an adjacent hyalocyst. The pressure transducer was calibrated at 14.27 mV/MPa.

The diameter of the capillary opening is critical. Small diameter probe tips clog with debris, or the oil-water meniscus fails to move freely when the interior wall of the tip is coated with debris from the water. A large probe opening results in difficulty controlling the oil-water meniscus because the resistance due to friction is too small and often leads to flooding of the sample with oil from the probe. Internal tip diameters of 2 to 3 μm were a good compromise for this study, and tips were replaced after every one or two probe attempts.

Frequent replacement of the capillary tips also lessened the incidence of bubbles developing within the oil. Breaks in the integrity of the oil were only seen after debris had collected on the capillary wall or after a bubble was inadvertently allowed into the oil column. The breaking point of oil in a clean probe tip is not known, but must occur at lower pressures than were achieved in the probed hyalocysts.

To ready the capillary tip for a probe, a small amount of lumen water is withdrawn into the the capillary by suction created by backing off the thumbscrew control. For lumen pressure measurements, the visible oil-water meniscus must be held stationary during dehydration by manually manipulating the thumbscrew. The accuracy of a lumen pressure measurement depends in part on the experimenter's ability to maintain the position of the meniscus. Several factors cooperate to make that task difficult. The meniscus moves towards the probe tip as lumen pressure decreases, and vibration and minor fluctuations in ambient temperature cause the meniscus to vacillate. The difference between the pressure at full hydration and the pressure at bubble entry is ΔP.

A variety of other technical problems can occur during a probe (cf., Nonami et al., 1987). The difficulties of manipulating the oil-water meniscus and accidental flooding of the sample with probe oil have already been mentioned. Because of tissue movement during dehydration or because of vibration, the capillary tip can pull out of the pore, or abut or push through the opposite hyaline wall. Any of these can occur at any time in the course of a probe and will adversely affect results. At least one of them usually did occur, so that the oil-water meniscus, the tip of the probe, and the air-water meniscus

all had to be carefully monitored during a probe. Only those probes with no known complications were used in the analysis. This yielded 8 data points from about 50 measurements and as many aborted attempts.

An additional 4 measurements were taken from leaves that were wetted with a 0.1% (v/v) solution of the detergent TWEEN-80 in distilled water. The detergent should reduce the pressure differential required to pull a mensicus through a pore by lowering the surface tension at the air-water interface. When wetting a leaf with this solution, enough of the solution was applied to approximately double the volume of water already present in and on the leaf. Although the concentration of TWEEN-80 at bubble entry is not known, it should be close to or slightly below that of the applied solution when enough water evaporates for menisci to develop in the pores of the hyalocysts. The surface tension ($T = F/l$, where F is the force on a wire of length l) of the 0.1% solution of TWEEN-80 was estimated by measuring the force required to pull a 1 cm long straight wire, which was oriented parallel to the surface of a pool of solution, free from the liquid. The surface tension of distilled deionized water was also measured using the same technique. The experimental value for distilled deionized water was 11% lower than the accepted value for the surface tension of water at the same temperature (Weast, 1968). To correct for the error in our technique, the difference between the experimental and the established value for the surface tension of water was used to correct the experimental value for the surface tension of 0.1% TWEEN-80.

Pore Diameter Measurements. Following a lumen pressure measurement, the diameter of the pore through which the bubble entered

was measured with an ocular micrometer. The few elliptical pores were only slightly eccentric, thus were taken to be circular. For use in Equation 2, a better approximation for the pore diameter of more elliptical pores may be given by the hydraulic diameter (Appendix).

RESULTS AND DISCUSSION

Excised leaves exposed to air dehydrate within a few minutes. Leaves which are rehydrated by the addition of water from a pipet or syringe return to almost complete hydration in seconds. All fully hydrated hyalocysts (i.e., those with no air bubbles visible in their lumens) embolized by air-seeding. The meniscus entered each lumen through the pore with the largest diameter unless that pore was obstructed. Figure 2.4 depicts an air-seeding sequence. The air-water meniscus in the pore at the arrow is just developing in Figure 2.4A as the leaf surface water dissipates. The meniscus is visible in the lumen in Figure 2.4B. Its diameter approximates that of the pore. In Figure 2.4C, the meniscus pulls into the hyalocyst and looks bubble-like within the lumen. In Figure 2.4D, the bubble expands to embolize the cell. When a meniscus pulled through a hyaline pore, bubbles in nearby cells contracted slightly, then continued to expand as evaporation proceeded. This localized relief of tension was common, but short-lived.

The only hyalocysts which did not air-seed had entrapped bubbles

at the onset of dehydration. Figure 2.5, lower arrow, shows a bubble which begins to collapse when the leaf is wetted, but as dehydration begins before the bubble completely collapses, it expands, eventually filling the hyalocyst. This cell embolizes without air-seeding. On one occasion, a hyalocyst with an entrapped bubble air-seeded. In this case, the entrapped bubble was separated from the rest of the cell by a spiral thickening which closed the connecting passage to a diameter less than that of the pore through which the air-seed entered. Measurement of lumen pressures in hyalocysts with entrapped bubbles is not feasible with present techniques.

In Figure 2.6, lumen pressure measurements of air-seeded cells wet with tap water (solid dots) correspond well with the predicted curve (solid line). Those wet with tap water and TWEEN-80 (open circles) air-seed at tensions lower than predicted by Equation 2 because the detergent lowers the surface tension of the meniscus from 7.2×10^{-2} N/m (water at 20^{o}C) to about 4.3×10^{-2} N/m at bubble entry, and thus lowers the pressure differential (dotted line) required to deform the meniscus enough to fit through the pore. The TWEEN-80 curve is intended to demonstrate the lowering of the surface tension, not to represent a curve that should fit the experimental data.

As Huber (1956) suggested, *Sphagnum* hyaline cells may be a good model for the air-seeding of fern annuli. They may also be a good model for the air-seeding of tracheary elements, as Zimmermann (1983) suggested. Perhaps the model is even more appropriate in the case of tracheary elements because both they and *Sphagnum* hyalocysts are no longer living and when hydrated contain water almost exclusively. The pores in the pit membranes of tracheary elements may be comparable to

hyaline pores in that they prevent air from entering the lumen until a critical pressure differential across the pore is reached. There is evidence that *Sphagnum* hyalocysts are an appropriate model for xylem elements in other respects. In both hyalocysts and xylem elements, released water increases the hydration of adjacent cells (Dixon, et al. 1984). There is also mounting evidence that tracheary elements will air-seed more than once if completely rehydrated after drying, but that those elements with entrapped bubbles do not air-seed (Lewis and Tyree, unpublished data). But whatever the outcome of the xylem investigations, we now have confident measurements to indicate that the capillary equation does describe the behavior of air-seeding in plants, particularly in *Sphagnum*.

APPENDIX

In general, the capillary equation says that the upward component of force which raises the water in a capillary tube is equal to the weight of the water supported at equilibrium. The force acts on the water through the surface tension of the air-water meniscus as the water adheres to the tube wall. Thus, in the case of a circular tube of internal diameter a, $(\pi a)(T \cos\Theta) = (\pi a^2/4)(h)(sg)$, where πa is the perimeter of the tube, $T \cos\Theta$ is the upward component of the force exerted by the surface tension T through the contact angle Θ between the water and the tube, and the weight of the supported water is given by the cross-sectional area of the tube $\pi a^2/4$ multiplied by the height of the water column h, the density of water s, and the acceleration due

to gravity g. Rearranging gives hsg = (4T cosθ)/a. Since T and cosθ are constants and hsg is the negative of the pressure drop across the meniscus, the pressure differential ΔP in the case of a cell dehydrating, ΔP = 0.29/a where ΔP is in MPa and a is in μm.

For a tube with rectangular cross-section, $2(a+b)(T \cos\theta) = (ab)(h)(sg)$ where a and b are the width and length of the rectangle. Rearranging gives $hsg = (4T \cos\theta)/(2ab/(a+b))$. Substituting the constants and correcting for units gives $\Delta P = 0.29/(2ab/(a+b))$. If a = b, then $\Delta P = 0.29/(2a^2/2a) = 0.29/a$. The pressure required to pull the meniscus through a square tube of width a is the same as for a circular tube of diameter a. If a << b, then $\Delta P \tilde{=} 0.29/(2ab/b) \tilde{=} 0.29/2a \tilde{=} 0.15/a$ (Pickard's [1981] equation for parallel plates). For wide parallel plates separated by distance a, the pressure required to pull the meniscus through the plates is one-half the pressure required to pull the meniscus through a circular tube of diameter a (Fig. 2.7).

The perimeter of an ellipse is approximated by $\pi((a^2+b^2)/2)^{1/2}$, and the area is given by $\pi ab/4$ (Eves, 1974), thus $(\pi((a^2+b^2)/2)^{1/2})(T \cos\theta) \tilde{=} (\pi ab/4)(h)(sg)$, where a and b are the axes of the ellipse. Rearranging, yields $hsg \tilde{=} (4T \cos\theta)/(2a^2b^2/(a^2+b^2))^{1/2}$; substituting for constants and correcting for units gives $\Delta P \tilde{=} 0.29/(2a^2b^2/(a^2+b^2))^{1/2}$. If a = b, then $\Delta P \tilde{=} 0.29/(2a^2a^2/(2a^2))^{1/2} \tilde{=} 0.29/a$, the pressure required to pull a meniscus through a circular tube of diameter a. When a << b, $\Delta P \tilde{=} 0.29/(2a^2b^2/b^2)^{1/2} \tilde{=} 0.21/a$. In a tube with an elongated elliptical cross-section and minor axis of length a, the pressure differential required to pull the meniscus through the tube is about

7/10ths the pressure required to pull the meniscus through a circular tube of diameter a (Fig. 2.7).

Note that for a rectangular tube and for an elliptical tube, the terms $2ab/(a+b)$ and $(2a^2b^2/(a^2+b^2))^{1/2}$, respectively, are the hydraulic diameters. The hydraulic diameter of a regularly shaped conduit is the diameter of the circular conduit that has the same rate of flow at the same pressure gradient (i.e., it is the geometric diameter of the hydraulically equivalent circular conduit) (Li and Lam, 1964). Hydraulic diameter is calculated by $d = 4A/p$, where A and p are the area and the perimeter of the conduit.

LITERATURE CITED

Bailey IW 1916 The structure of the bordered pits of conifers and its bearing upon the tension hypothesis of the ascent of sap in plants. Bot Gaz 62: 133-142

Clymo RS, PM Hayward 1982 The ecology of *Sphagnum*. *In* AJE Smith, ed, Bryophyte Ecology. Chapman and Hall, London, New York, pp 229-289

Cosgrove DJ 1985 Cell wall yield properties of growing tissue: evaluation by *in vivo* stress relaxation. Plant Physiol 78: 347-356

Crombie DS, MF Hipkins, JA Milburn 1985a Gas penetration of pit membranes in the xylem of *Rhododendron* as the cause of acoustically detectable sap cavitation. Aust J Plant Physiol 12: 445-453

Dixon MA, J Grace, MT Tyree 1984 Concurrent measurements of stem density, leaf and stem water potential, stomatal conductance and cavitation on a sapling of *Thuja occidentalis* L. Plant Cell and Environ 7: 615-618

Eves H 1974 Geometry: mensuration formulas. *In* WH Beyer, ed, CRC Standard Mathematical Tables, Ed. 27. CRC Press Inc, Boca Raton FL, p 124

Huber B 1956 Die Gafässleitung. *In* O Stocker, ed, Encyclopedia of Plant Physiology. Springer, Berlin, Göttingen, Heidelberg, pp 541-582

Hüsken D, E Steudle, U Zimmermann 1978 Pressure probe technique for measuring water relations of cells of higher plants. Plant Physiol 61: 158-163

Li W-H, S-H Lam 1964 Principles of Fluid Mechanics. Addison-Wesley Publishing Co, Reading MA, Menlo Park CA, London, Amsterdam, Don

Mills ONT, Sydney, p 276

Nonami H, JS Boyer, E Steudle 1987 Pressure probe and isopiestic psychrometer measure similar turgor. Plant Physiol 83: 592-595

Oertli JJ 1971 The stability of water under tension in the xylem. Z Pflanzenphysiol 65: 195-209

Pickard WF 1981 The ascent of sap in plants. Prog Biophys molec Biol 37: 181-229

Renner O 1925 Die Porenweite der Zellhäute in ihrer Beziehung zum Saftsteigen. Ber dtsch bot Ges 43: 207-211

Sperry JS, NM Holbrook, MH Zimmermann, MT Tyree 1987 Spring filling of xylem vessels in wild grapevine. Plant Physiol 83: 414-417

Tyree MT, MA Dixon 1986 Water stress induced cavitation and embolism in some woody plants. Physiol Plant 66: 397-405

Weast RC, ed 1968 CRC Handbook of Chemistry and Physics. The Chemical Rubber Co., Cleveland OH, p F-30

Zimmermann MH 1983 Xylem Structure and the Ascent of Sap. Springer-Verlag, Berlin, Heidelberg, New York, Tokyo

Fig. 2.1. Photomicrograph of abaxial surface of *Sphagnum* leaf showing chlorophyllous cells (a), and a complete hyalocyst (b) with hyaline pores (c) and spiral thickenings (d) on the interior of the hyaline wall. Scale = 50 μm.

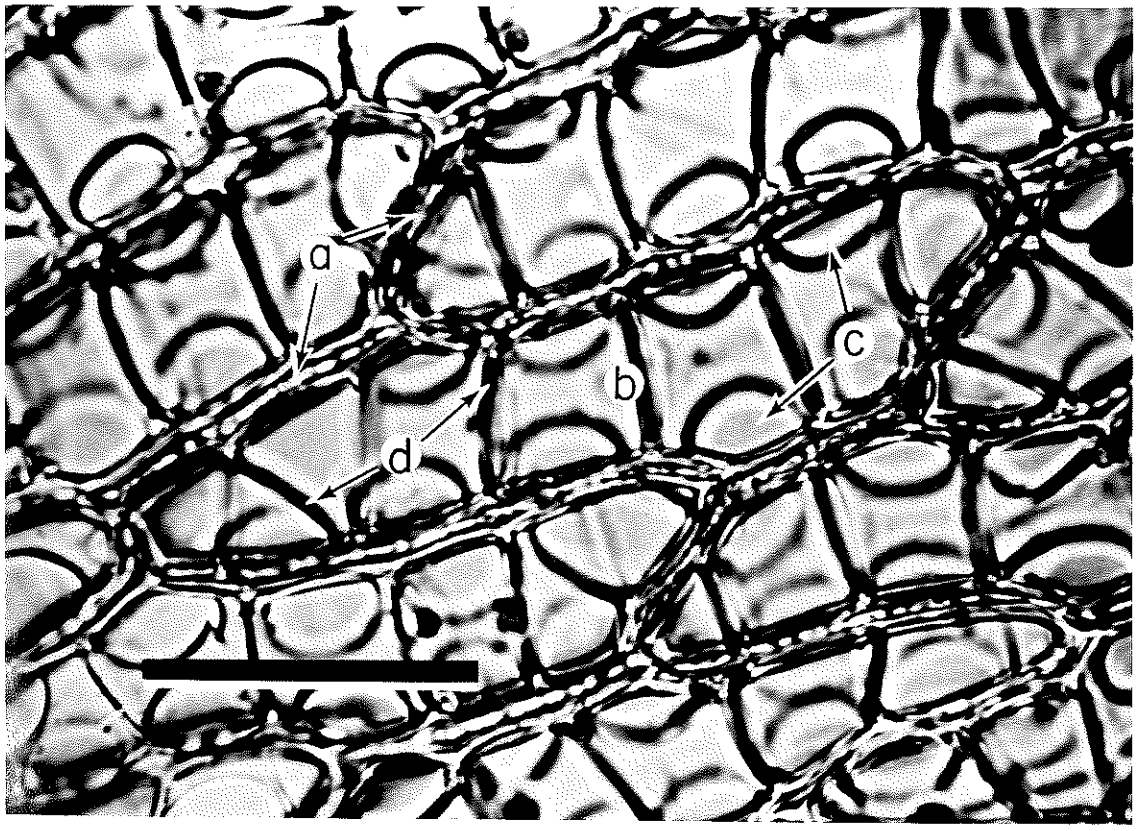
a
b
c
d

Fig. 2.2. Scanning EM of pores in *Sphagnum* hyalocyst. The pores are perforations in the cell wall which connect the cell's exterior to the lumen of the cell. A mature hyalocyst is dead; the lumen contains no protoplasm. Scale = 50 μm.

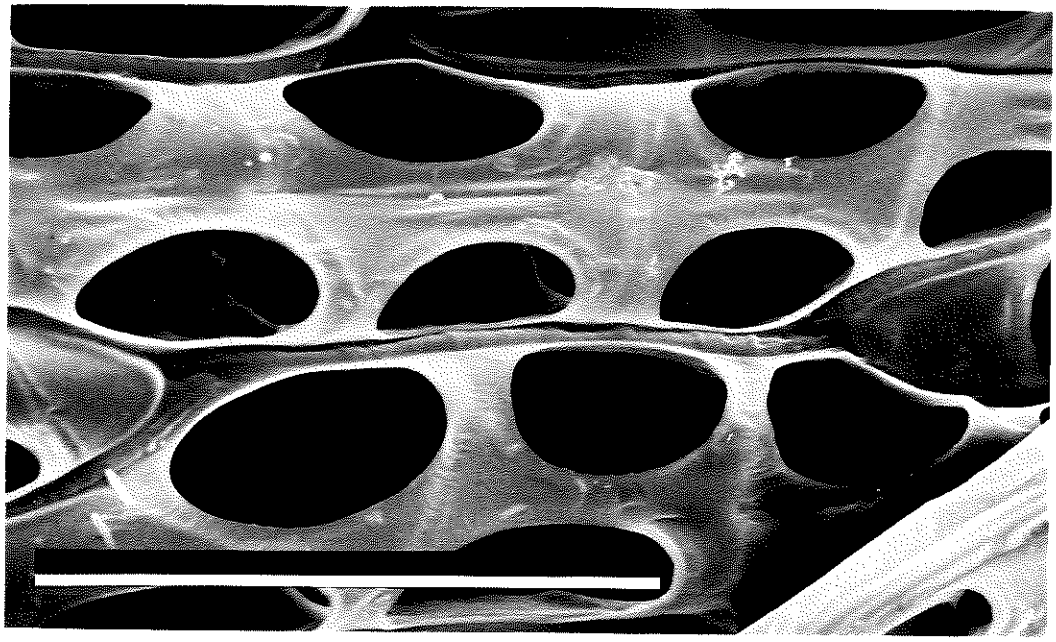

Fig. 2.3. Pressure microprobe set-up. A, Microprobe apparatus. B, Microprobe inserted into hyalocyst.

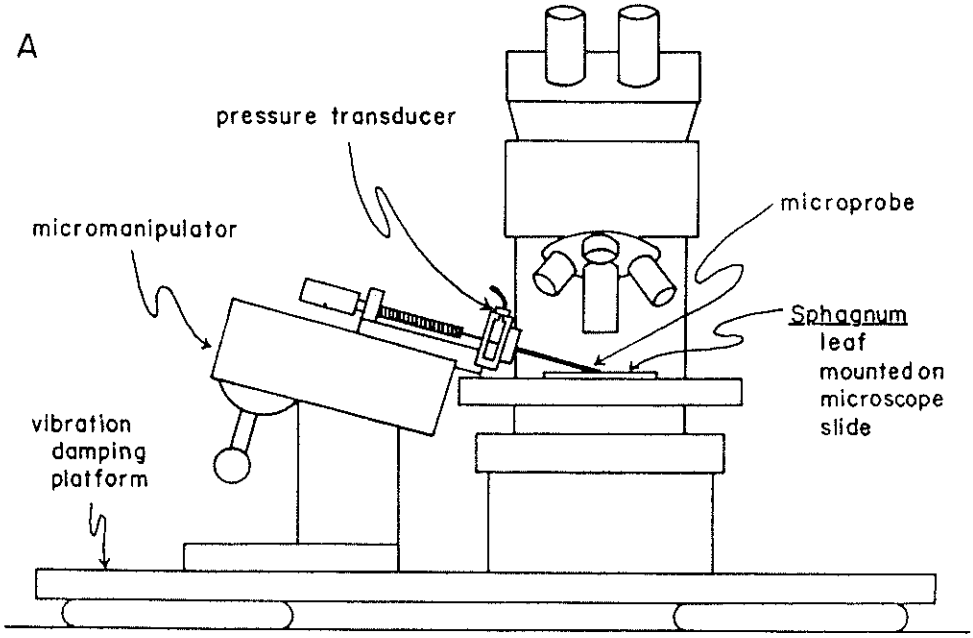
A
pressure transducer
micromanipulator
microprobe
Sphagnum leaf mounted on microscope slide
vibration damping platform

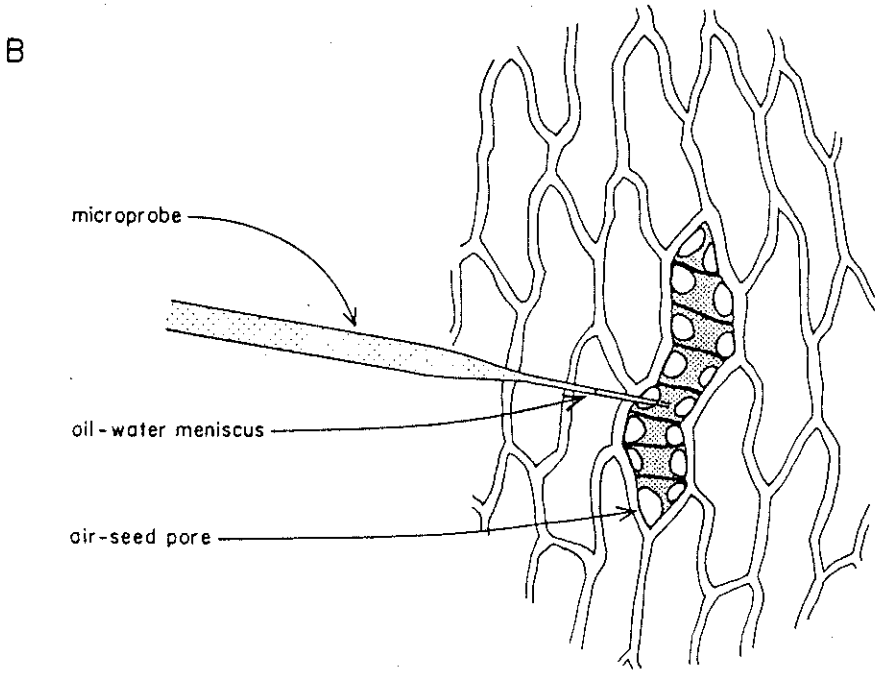
B
microprobe
oil-water meniscus
air-seed pore

Fig. 2.4. Air-seeding hyalocyst. The photomicrographs are accompanied by line drawings of the hyalocyst for clarity. A, The pore through which the air-seed enters. B, The meniscus is visible in the cell lumen. The meniscus diameter has diminished until it approximates the diameter of the pore. C, The meniscus has pulled through the pore and begins expansion. After the diameter of the meniscus has decreased to that of the pore, allowing bubble entry, the meniscus increases its diameter. This expansion takes place within the hyalocyst lumen. The hyalocyst has air-seeded. Note that other hyalocysts are in different phases of air-seeding. D, The bubble expands to fill the cell. The cell is embolized.

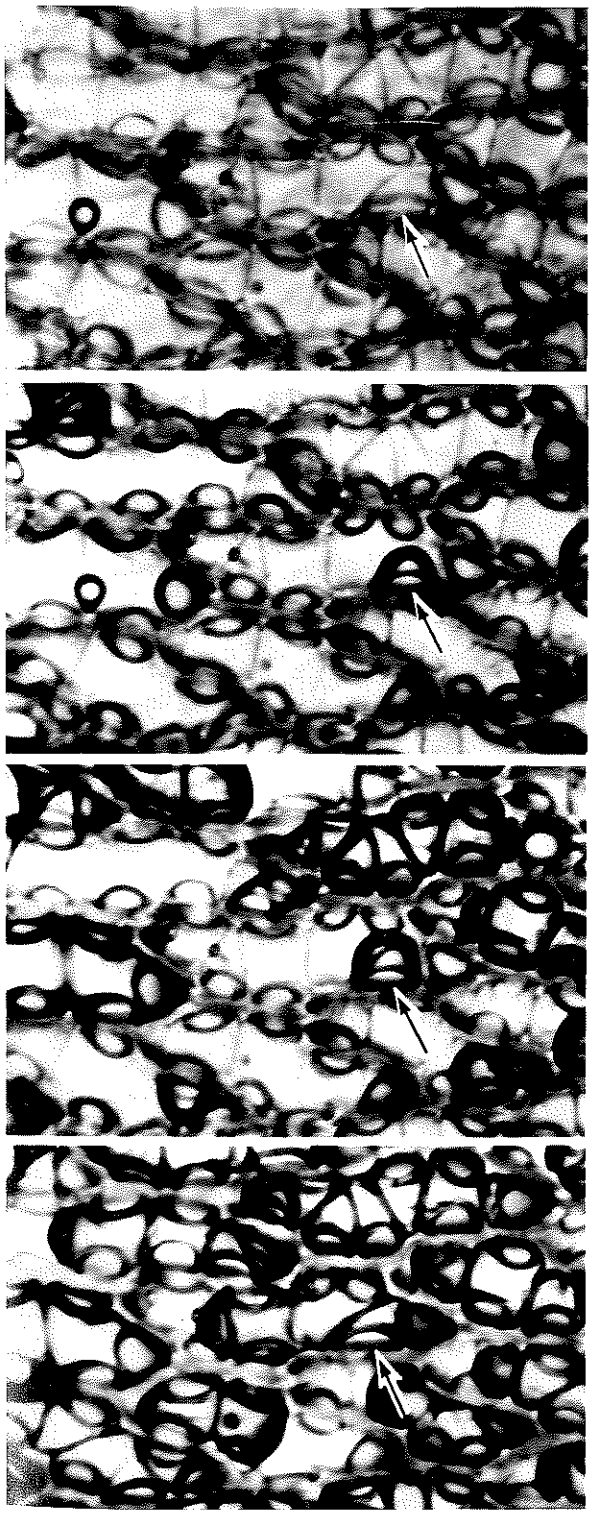
A
B
C
D

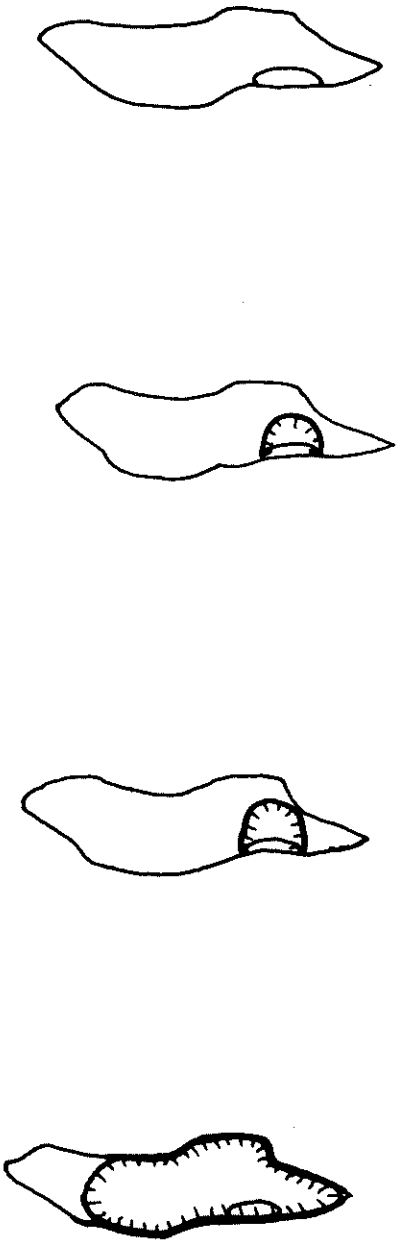

Fig. 2.5. Embolism by expansion of an entrapped bubble. In this sequence photographed from a video screen, the leaf has been rewetted after dehydration. A, Many hyalocysts contain entrapped bubbles formed during rewetting. B, The bubble in the cell indicated by the upper arrow has collapsed. The bubble in the cell indicated by the lower arrow shrinks, but does not completely dissolve before dehydration begins again. C, The bubble in the lower cell expands leading to embolism. D, The upper hyalocyst air-seeds.

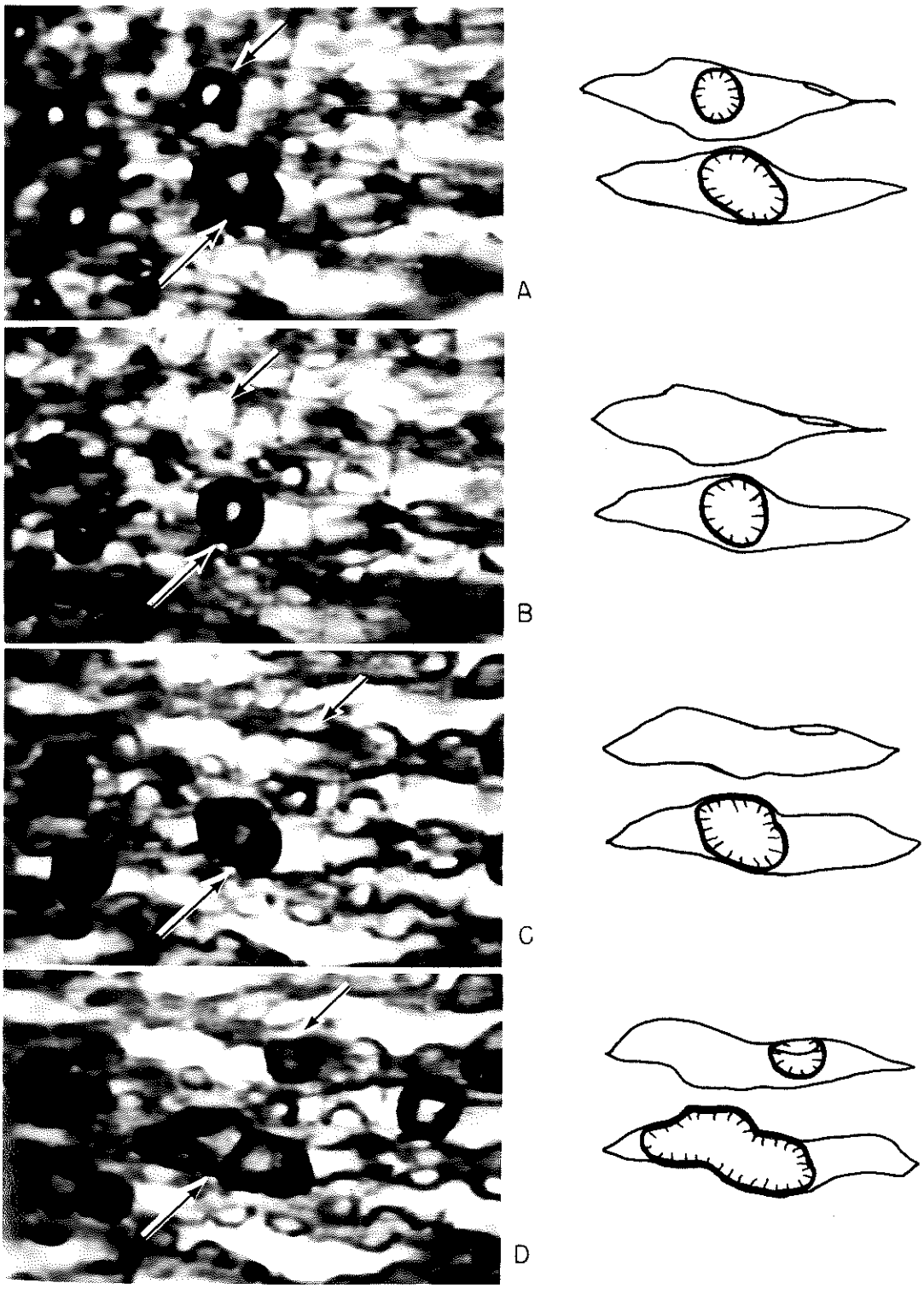
A
B
C
D

Fig. 2.6. Lumen pressures at air-seeding. Hyalocyst lumen pressures were measured at the instant of air-seeding with the pressure microprobe. Tension is pressure below ambient (0.1 MPa) and is plotted against the pore diameter, which, in the case of elliptical pores, is corrected to the hydraulically equivalent circular pore diameter (see text). In most pressure measurements leaves were wet with tap water(●). Leaves wet with 0.1% (v/v) TWEEN-80 in tap water (o) air-seeded at smaller pressure differentials. The solid line is the predicted curve for leaves wet with water at 20^{o}C. The dotted line is the predicted curve for leaves wet with TWEEN-80 at the same temperature.

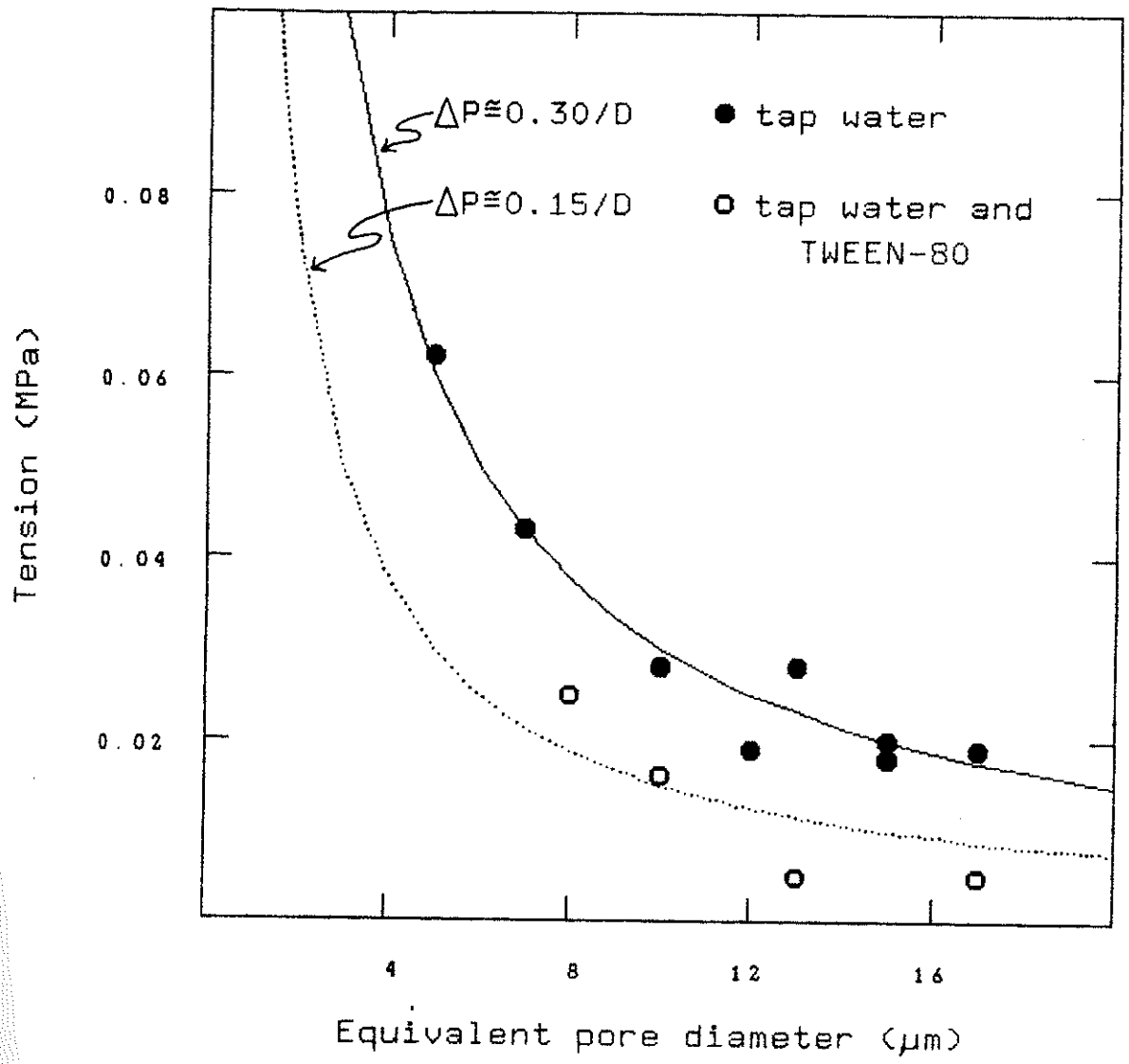
ΔP≅0.30/D
ΔP≅0.15/D
tap water
tap water and TWEEN-80
0.08
0.06
0.04
0.02
Tension (MPa)
4
8
12
16
Equivalent pore diameter (μm)

Fig. 2.7. Pressure differential (ΔP) in elliptical and rectangular conduits for a range of major axis lengths when the minor axis has a length of 1 μm. For both elliptical and rectangular conduits, when the major and minor axes are of equal length, ΔP is the same as that for a circular conduit, 0.29 MPa. As the difference between the major axis and minor axis lengths increases, ΔP decreases. The decrease reaches a limit at approximately 0.21 MPa for an elliptical conduit and 0.15 MPa for a rectangular conduit.

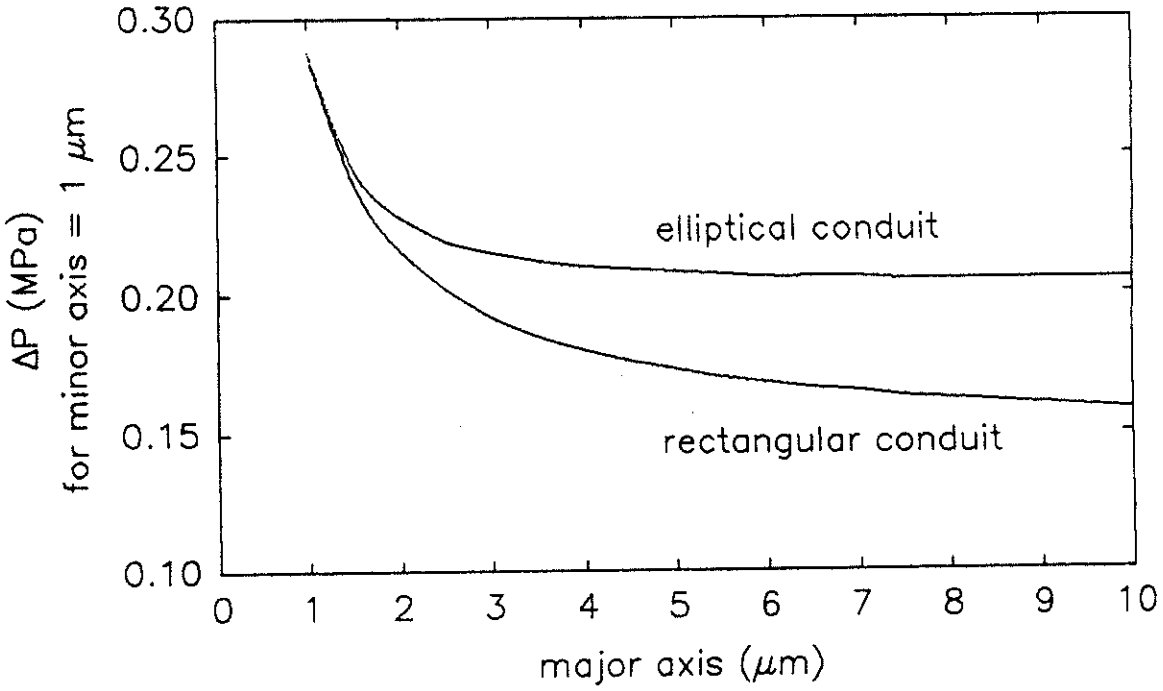
0.30
0.25
0.20
0.15
0.10
ΔP (MPa)
for minor axis = 1 μm
elliptical conduit
rectangular conduit
0
1
2
3
4
5
6
7
8
9
10
major axis (μm)

CHAPTER 3

Acoustic Emissions are Good Indicators of Cavitation in *Thuja occidentalis* Tracheids Under Water Stress[1]

INTRODUCTION

In order to understand the details of embolism in the xylem, it is necessary to have a means of measuring the formation of emboli by a non-intrusive method. Assuming that cavitations lead to embolism, Milburn and Johnson (1966) and Crombie et al. (1985) used "clicks" produced by dehydrating plants as indicators of cavitation in tracheary elements in studies of the water relations of *Ricinus*, *Plantago*, and other genera. They measured sounds emitted in the audible frequencies (0.2 to 1.0 kHz [kilohertz] [as cited in Milburn, 1973]), a procedure which requires a soundproof specimen holder or sampling room and restricts manipulation of the plant material and surrounding apparatus. Tyree has since developed the technique of measuring emissions in the ultrasonic frequencies, 100 kHz to 2 MHz (megahertz) (Tyree and Dixon, 1983). The use of ultrasonic emissions has the advantages of eliminating most background noise and allowing for limited manipulation

---

[1] This chapter is intended for submission to an as yet unspecified journal.

of the sample even while acoustic emissions (AEs) are monitored.

The use of AEs to indicate the occurrence of xylem cavitations as precursors of embolism is justified because AEs coincide with water loss in tissue dehydrating under tension (Milburn, 1973; Dixon et al., 1984) and with the loss of xylem conductance (Sperry, 1986). Furthermore, there is approximately a one-to-one correspondence between the number of tracheids in a sample of *Thuja occidentalis* wood and the number of AEs that are counted during dehydration of the initially fully hydrated sample (Tyree et al., 1984b).

Even though AEs have been used for several years in botanical research, there remain major unanswered questions about the emissions and their generation. Some answers are suggested by previous research, but too often reliable results are lacking. In this chapter, these questions are addressed for tracheids in *Thuja occidentalis* wood: Are AEs and the formation of emboli simultaneous? Are AEs produced when tracheids are embolized by forcing air into them under positive pressure? Does a tracheid produce an AE if it has a visible entrapped bubble at the onset of dehydration? Answers to these questions can help determine whether AEs can be used to indicate the formation of emboli in vascular elements of fully hydrated tissue. This research uses modified techniques which allow events during dehydration to be followed in smaller tissue samples than have been used previously. These methods more closely approximate the ideal: monitoring events on a tracheid by tracheid basis. The data confirm that ultrasonic AEs are good indicators for the occurrence of cavitation in *T. occidentalis* tracheids.

MATERIALS AND METHODS

Plant Material. Greenhouse-grown *Thuja occidentalis* L. plants were cut above the root collar, the cut surfaces were trimmed with a razor blade under tap water, and the shoots were rehydrated in 5 mM KCl in distilled deionized water. Both the tap water and the KCl solution were filtered to 0.7 µm and degassed to approximately -0.1 MPa under vacuum. All subsequent cuts, including those made during sectioning, were executed in a puddle or in a bath of untreated tap water. During rehydration, the plants were enclosed in a plastic bag and kept in the dark for at least 8 to 10 hours. Wood was considered "fully hydrated" when removed from shoots that were rehydrated in this manner. All stem sections used in experiments had 9 or fewer growth rings; most were 5 years old or less. Longitudinal sections were made with a sliding microtome, and the samples were trimmed to size with a razor blade under a dissecting microscope in order to make each longitudinal cut parallel to the tracheids. The dimensions of the plant material used in each set of experiments are described below.

T. occidentalis was selected for this study for several reasons. It is under investigation by other researchers in water relations. It has pit membranes with limited torus development. (It is thought that pit membranes in conifers with fully developed tori prevent air from passing from tracheid to tracheid by aspiration of the membranes: a nonporous torus seals against the pit aperture and blocks air passage. An aspirated pit membrane with a thickened torus complicates the determination of limiting pore diameter because the passage of air from

tracheid to tracheid may be limited by the space between the aspirated membrane and the pit wall rather than by perforations in the membrane.) The xylem of *Thuja occidentalis* wood lacks resin ducts, which makes manipulation simpler because resin does not clog cut tracheids; and fresh material was readily available.

Detection of Acoustic Emissions. AEs were detected with a 300 kHz transducer, 250 to 500 kHz filter, and an acoustic emission counter model 204B produced by Acoustic Emission Technology Corporation, Sacramento CA. In most experiments, the transducer was mounted in a holder made of plexiglas with a glass microscope slide base. The sample was covered with one of two plexiglas slips, and two spring steel clamps held the whole in place (Fig. 3.1). A conical hole was drilled through the plexiglas holder adjacent to the transducer to reduce interference with transmitted light. The narrow part of the hole had a diameter of 1 mm and was oriented toward the specimen. A corresponding 1-mm-diameter hole drilled in one cover slip provided an unobstructed view of part of the specimen and increased air circulation, thus decreasing dehydration times. When this cover slip was used, the hole in the cover slip overlapped the light transmission port. The other cover slip had an opening large enough to extend beyond the edges of both the basal hole and the transducer. This port was covered with fiberglass window screen in order to hold the sample firmly against the transducer, and to minimize gross movement during dehydration while allowing evaporation from the entire upper surface of the plant section.

In order to detect AEs produced by dehydration with positive pressure, the transducer was mounted on the stem segment inside of a

pressure bomb using a spring loaded clamp. The top of the bomb was modified to permit the transducer wire to exit through a separate opening. In all experiments, the cumulative count signal from the counter was recorded on a paper chart recorder equipped with an event marker.

Observation of Embolism. Radial and tangential sections, 30 to 90 μm thick, were observed under a compound microscope equipped with a 32X long-working-distance objective (working distance = 6.6 mm). Total magnification was 320X. Care was taken to select sections for study that were as parallel to the tracheids as possible. In a given segment, the long dimension refers to the segment length in the axial direction. For simple observation, a section measuring approximately 1.0 cm by 0.5 cm by 45 or 60 μm was held securely on a microscope slide under a cover slip or mounted in the transducer holder. When a cover slip with a viewing port was employed, an unobstructed view through a hole in the screen or through the 1-mm port was possible once most of the free water evaporated. Recordings on video tape for play-back at slow speeds were made through the microscope phototube using the same arrangements.

In order to compare the timing of emboli formation with the production of AEs, a 30 or 60 μm thick longitudinal section was mounted on the transducer in its holder using the cover slip with the screen insert. Most of the 1.5 cm length rested on the transducer; the remainder overlapped the port by at least 1.5 mm, so that the view did not include tracheids that were cut transversly at the end of the section. Section widths ranged from 2 to 8 mm. After focusing the 32X objective through the screen, the occurrence of events observed through

the microscope during dehydration of the sample was superimposed on the chart recorder tally of cumulative AEs with an event marker.

Detection of Cavitation During Dehydration Under Positive Pressure. A fully hydrated stem segment measuring 10 cm in length was debarked and inserted into a pressure bomb leaving the apical 1 cm of length exposed on the outside of the bomb. The AE transducer was attached to the portion of the stem inside of the bomb. Bomb pressure was raised gradually over several minutes to 5.4 MPa. The experiment was repeated, raising the pressure more quickly to the maximum.

RESULTS

No bubbles were visible within the tissue when longitudinal sections from fully hydrated *Thuja occidentalis* stems were examined under a light microscope at 320X. In tissue that was dehydrated from full hydration, a sequence of events was noted:

1) Menisci could be seen forming at the cut surfaces of tracheids in the outer parts of the section and retreating along each cut tracheid as drying proceeded (Fig. 3.2A).

2) Menisci moved more quickly through tracheids in deeper layers of the section. Because cuts could not be made perfectly parallel to all tracheids during sectioning, it is assumed that tracheids with more slowly moving menisci extended to the surface of the section and were cut or cracked during

sample preparation. A meniscus should enter a tracheid through a small puncture, after dehydration has progressed enough to develop a greater tension in the lumen than would build in a tracheid with a larger cut. Presumably, the higher tension creates more instability in the water column, resulting in more rapid embolus development when the water column finally breaks.

3) Menisci moved through deep tissue layers at much greater speeds than in the previous steps (Fig. 3.2B). Through time, the average rate at which the menisci moved through the section increased to such an extent that an individual meniscus could not be followed by eye, but the direction of its movement usually could be discerned. Sometimes these rapid movements were discernible only as rapid transparency changes within the tracheids. Analysis at lower magnifications (60 to 100X) and in slow motion on video tape shows that a meniscus is present. Occasionally, a much more slowly moving meniscus is visible during this stage; slow moving menisci become more common toward the end of this phase. Rarely, a short time exists when only a few slowly moving menisci are visible. The very fast meniscus movements occur when a tracheid cavitates. Rapid expansion of the air bubble that pulls through a pore proceeds as the air behaves as an ideal gas to increase its volume in proportion to the pressure difference between the surrounding air and the tracheid lumen (Boyle's Law). Simultaneously lumen water

evaporates into the bubble. With the rapid rise in lumen pressure at bubble entry, some of the lumen water is released to neighboring cells, as demonstrated by vacillations of visible menisci in nearby lumens. The slower moving menisci seen in tracheids at this time are the boundaries of bubbles that a few instants earlier would have been seen in other parts of the same tracheids as quickly moving menisci. Once the initial rapid pressure equilibration is complete, the retreat of free water in a cavitated lumen proceeds more slowly.

4) No more menisci are seen. Tracheid walls become more and more opaque, and the section has a greater tendency to move. When the menisci are gone, all tracheids are embolized, but translucence in the walls indicates that the walls are still hydrated. Opaque walls signal fully dehydrated tissue.

5) All movement stops.

The time required for completion of this series of events depends on the presence of a cover slip, the ambient relative humidity, the temperature of the microscope lamp, and the presence of drafts. In the absence of a cover slip, the complete sequence occurred in less than 5 to 10 min.

Tissue that was dehydrated just until no free water was visible within the tissue at 320X, then rehydrated by placing the section in a puddle of water for a few minutes, had bubbles visible within some

tracheids (Fig. 3.3). Most of these bubbles slowly collapsed in the next 15 to 30 min. In sections that were dehydrated for an hour or more, the tracheid walls were dry. Even when these fully dehydrated sections were rehydrated overnight, they had more embolized tracheids than did partially dehydrated tissue that was rehydrated for one-half hour. Following dehydrations in which the tracheid walls do not dry, bubbles that form upon rewetting contain low concentrations of air. These bubbles collapse quickly when sufficient water is available. Bubbles that form upon rewetting of tracheids with dry walls contain little water vapor and are air primarily. Collapse of these bubbles requires long periods of rehydration.

An embolus forms in a tracheid in which a bubble is visible after rehydration by gradual expansion of that bubble. Fewer AEs are detected during dehydration of a section which is only partially rehydrated than are detected during the dehydration of the same section from full hydration (Fig. 3.4). Overnight rehydration of that same section returns the cumulative count of AEs to near that of the original, as long as dehydration has not proceeded long enough for the tracheid walls to dry. Cumulative AE counts after very long dehydrations do not return to original levels even with long rehydrations. Structural damage probably occurs to either the pit membranes, which are relatively flimsy structures, or to the cell walls of the tracheids. The damage could be tears caused by the tissue shrinkage that occurs at the end of long dehydrations due to the removal of water molecules from the cellulose microfibril network, or it could be other irreversible structural changes to the network, such as fibrillar realignments, caused by the removal of water. In these

instances, AEs may not occur during the course of the second dehydration even if the lumens completely refilled.

Figure 3.5 shows that no ultrasonic AEs register when menisci are seen to enter cut tracheids. The greatest rate of AE production occurs during the third stage of dehydration, when the menisci are moving most rapidly. AEs stop accumulating when the rapid meniscal movement stops. It is important to note that AEs are not generated by gross tissue movement; the rate of AEs drops to zero before the most noticeable tissue movement begins. Ultrasonic AEs are not generated by the expansion of free-floating entrapped bubbles in tracheids.

DISCUSSION

Embolus formation in superficial tracheids of *T. occidentalis* longitudinal sections and in *Sphagnum* hyalocysts is less energetic (visibly less abrupt) than that in deeply embedded tracheids. *Sphagnum* hyalocysts have pores in the cell wall with diameters of the same order of magnitude as the cut openings in the *T. occidentalis* tracheids. Ultrasonic AEs definitely attributable to embolism were not detected during the dehydration of hyalocysts, although a few emissions in the audible range with amplitudes just above that of the background noise were detected (Lewis and Tyree, unpublished data). Apparently, ultrasonic AEs are created by events that lead to rapid movements of menisci in tracheids. These energetic events are defined as cavitations (Chap. 1).

No ultrasonic AEs above the background count were detected during

pressurization of stem segments to over 5.0 MPa whether the pressure was raised slowly or quickly. AEs accumulated whenever the bomb pressure was released to approximately 1 MPa lower than the maximum pressure to which the sample was exposed. The interpretation of this is as follows: Dehydration by positive pressure does not cause energetic bubble formation in tracheids. Perhaps, during pressure bomb dehydration, an embolus forms by the entry of one or more small bubbles, each of which expands under the influence of Boyle's Law (ideal gas expansion: gas volume is inversely proportional to absolute pressure), until all lumen water is pushed out of the cell (the air-seeding hypothesis, using a broad interpretation). The final volume of the embolus should be proportional to the pressure differential across the meniscus at bubble entry unless the lumen volume is smaller. Lowering the bomb pressure from its maximum value creates a pressure differential across the menisci in the pores of tracheids into which bubbles have not previously entered, and causes water in these tracheids to cavitate by one of the mechanisms discussed. When tissue air dehydrates on the countertop, a single external air bubble enters the lumen and expands rapidly (a strict interpretation of the air-seeding hypothesis). The rate of bubble expansion determines whether AEs are produced. Rapid expansion produces detectable ultrasonic AEs; slow expansion does not produce detectable ultrasonic AEs.

Tyree (personal communication) proposes that the rapidity of expansion is limited in pressure bomb dehydration because most of the stem segment is enclosed in the bomb and is under pressure. The external force on a tracheid's walls pushes them towards the center of the tracheid. Bubble entry does not release this pressure, and the

pressure prevents the walls from rebounding when a bubble enters the lumen. In order for the bubble to expand, water must exit the lumen. The only space into which large amounts of released water can exit is in the portion of the stem segment exposed outside of the pressure bomb or into the air external to the bomb, so that the water released by bubble entry must travel or push other water over great distances to evacuate the volume that the bubble is to occupy. Tyree suggests that the resistance to water movement through this pathway is enough to prevent vibrations in the walls or the water in excess of 100 kHz. In order to produce an ultrasonic signal, the walls or the meniscus must experience maximum displacement in one-half of the time required to produce a full ultrasonic cycle, 5 μsec. In countertop dehydrations, there is no such external force on the tracheid walls. When a bubble enters a tracheid lumen, the tension is released, and, since there is no external compressing force, the walls return to the no tension condition, after bouncing in and out several times. Tyree believes that the initial wall displacement during rebound can occur in less than 5 μsec. This immediately frees part of the volume that the bubble will occupy, and water molecules travel only short distances with little resistance to immediately vacate the space for the bubble. He proposes that the vibration of the cell wall produces an AE.

A clearer picture of the mechanics of dehydration in wood is not yet available by the analysis of AEs because it is not yet clear how the interactions of pressure differentials and tissue anatomy and ultrastructure affect the characteristics (i.e., frequency, amplitude, and attenuation) of AEs. In fact, preliminary research by Tyree (personal communication) indicates that differences in the frequency

distribution of AEs between species are detectable but that the resonating characteristics of different AE transducers produce even greater variation. Knowledge of dehydration mechanics will be severely limited until more is known about AE production in dehydrating wood.

In summary, AEs are produced at the same time that embolus formation occurs in uncut tracheids of *Thuja occidentalis* wood. Fewer AEs are produced in wood that dehydrates with entrapped bubbles than in wood that dehydrates from full hydration. The number of AEs produced during dehydration can be restored to near maximum in the former case if the tissue is returned to full hydration, thus collapsing the entrapped bubbles, before the second drying commences. If dehydration proceeds to the point that the tracheid walls begin to dry, maximum AE counts cannot be restored or require much longer periods of rehydration than wood in which the walls retain their water.

LITERATURE CITED

Bailey IW 1916 The structure of the bordered pits of conifers and its bearing upon the tension hypothesis of the ascent of sap in plants. Bot Gaz 62: 133-142

Crombie DS, JA Milburn, MF Hipkins 1985b Maximum sustainable xylem sap tensions in *Rhododendron* and other species. Planta 163: 27-33

Dixon MA, J Grace, MT Tyree 1984 Concurrent measurements of stem density, leaf and stem water potential, stomatal conductance, and cavitation on a sapling of *Thuja occidentalis* L. Plant Cell Environ 7: 615-618

Huber B 1956 Die Gafässleitung. *In* O Stocker, ed, Encyclopedia of Plant Physiology. Springer, Berlin, Göttingen, Heidelberg, pp 541-582

Milburn JA 1973 Cavitation in *Ricinus* by acoustic detection: induction in excised leaves by various factors. Planta 110: 253-265

Milburn JA, RPC Johnson 1966 The conduction of sap: II, Detection of vibrations produced by sap cavitation in *Ricinus* xylem. Planta 69: 43-52

Sperry JS 1986 Relationship of xylem embolism to xylem pressure potential, stomatal closure, and shoot morphology in the palm *Rhapis excelsa*. Plant Physiol 83: 110-116

Tyree MT, Dixon MA 1983 Cavitation events in *Thuja occidentalis* L.?: ultrasonic emissions from the sapwood can be measured. Plant Physiol 72: 1094-1099

Tyree MT, MA Dixon 1986 Water stress induced cavitation and embolism in some woody plants. Physiol Plant 66: 397-405

Tyree MT, MA Dixon, EL Tyree, R Johnson 1984b Ultrasonic acoustic emissions from the sapwood of cedar and hemlock. Plant Physiol 75: 988-992

Zimmermann MH 1983 Xylem Structure and the Ascent of Sap. Springer-Verlag, Berlin, Heidelberg, New York, Tokyo

Fig. 3.1. Exploded diagram of the transducer holder for detecting ultrasonic emissions while viewing tracheids during dehydration. A longitudinal wood section contacts the transducer and covers the light transmission port when in place. The entire holder rests on the stage of a compound microscope, and the microscope objective can be focused through a hole in the screening of the cover shown. Alternatively, the ojective can be focused through a small hole (diameter = 1 mm) in another coverslip (not shown) which overlaps the light transmission port.

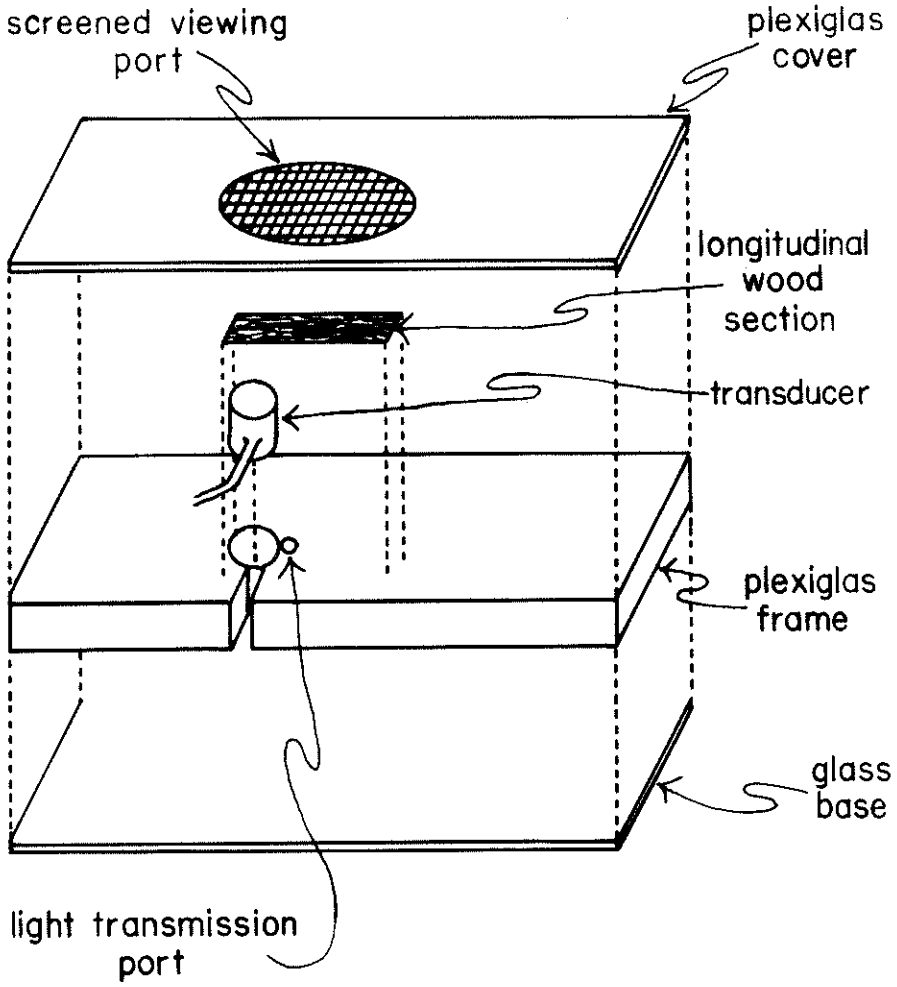
screened viewing port
plexiglas cover
longitudinal wood section
transducer
plexiglas frame
glass base
light transmission port

Fig. 3.2. Bubbles expanding in tracheids during dehydration. A, A bubble expands in a tracheid which was cut during sectioning. The cut is visible at the arrow in these photomicrographs. In the first frame the meniscus of the bubble is visible just above the cut tracheid wall. Frame 2, the meniscus moves through the tracheid. In Frame 3, the bubble has expanded and filled the lumen with air. In all three frames, menisci form at other holes in tracheid walls (especially at the far right of each frame). B, As in these diagrams, the walls of tracheids deeper in the tissue are not breached during sectioning and menisci expand rapidly to fill the lumens. The entire sequence shown from initiation to embolism, happens in less time than the sequence in A proceeds from the first to the second frame. At low magnifications, 60 to 100X, the bubbles are occasionally seen initiating at the walls.

A

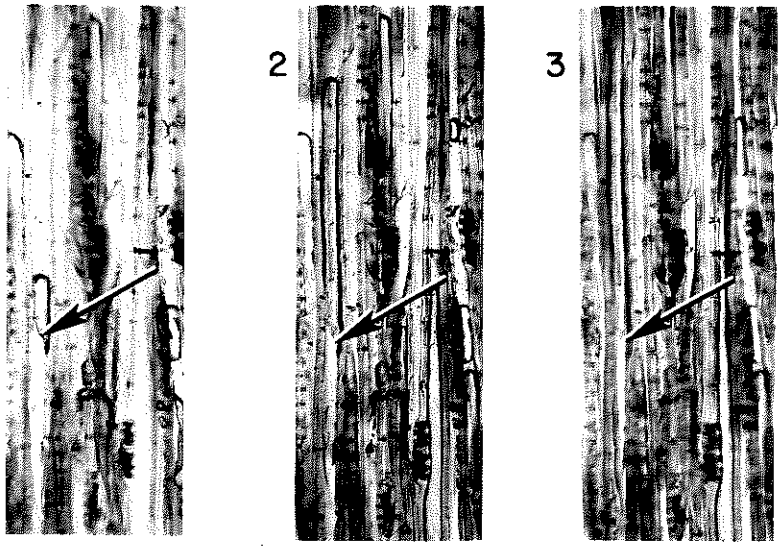

B

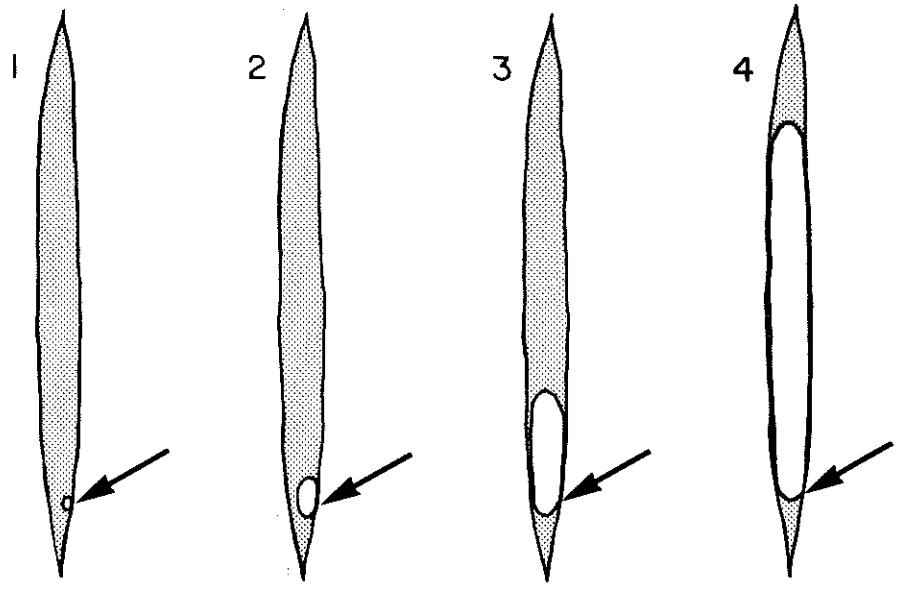

Fig. 3.3. Photomicrograph of entrapped bubbles in a longitudinal section of rehydrating tissue. This section was dehydrated until the tracheid walls were partially dry, then it was rewet with a few drops of water. After 5 min, some bubbles remain in the tracheids (a). Bubbles that were initially trapped have collapsed in some tracheids. Tracheids with no entrapped bubbles are fully rehydrated (b). The focus is set within the deeper tissue, so that the bubbles seen are trapped entirely within tracheid lumens. Scale = 100 μm.

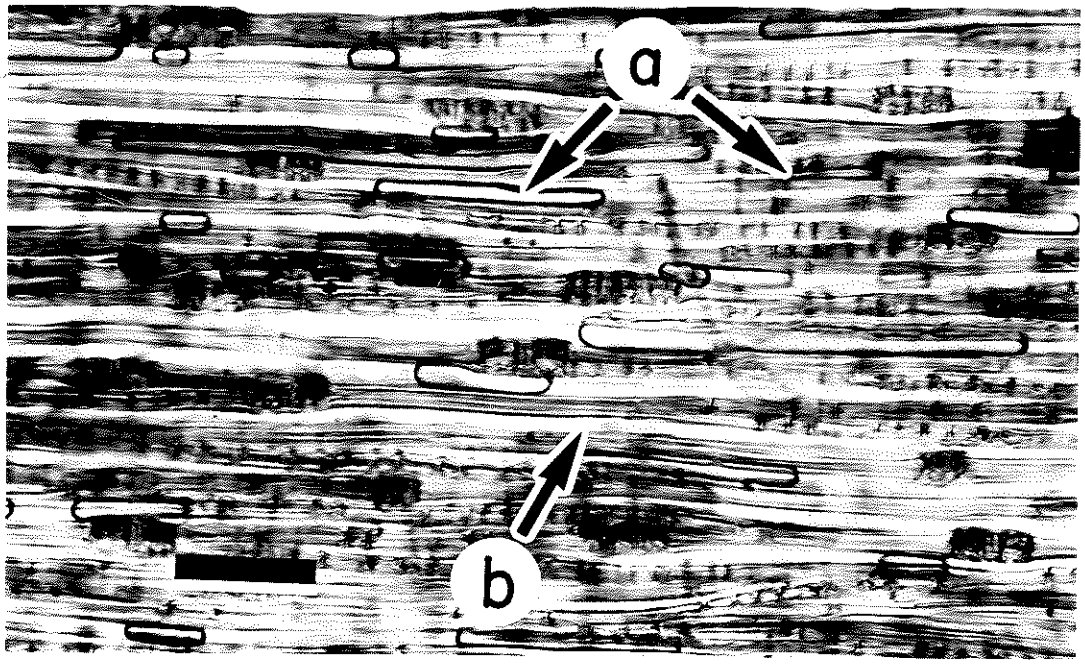
a
b

Fig. 3.4. Number of AEs detected during the second dehydration expressed as a percentage of the number of AEs produced during the first dehydration shown as a function of the rehydration time. These preliminary results were obtained by comparing the number of AEs produced during two dehydrations of the same tissue. Initially, fully hydrated longitudinal sections were dried for about 30 min (1st dehydration). They were rewet for about 5 min or 16 to 17 hours and dehydrated again (2nd dehydration). The number of AEs detected during the second dehydration as a percentage of the number of AEs detected during the initial dehydration is plotted against the rehydration time.

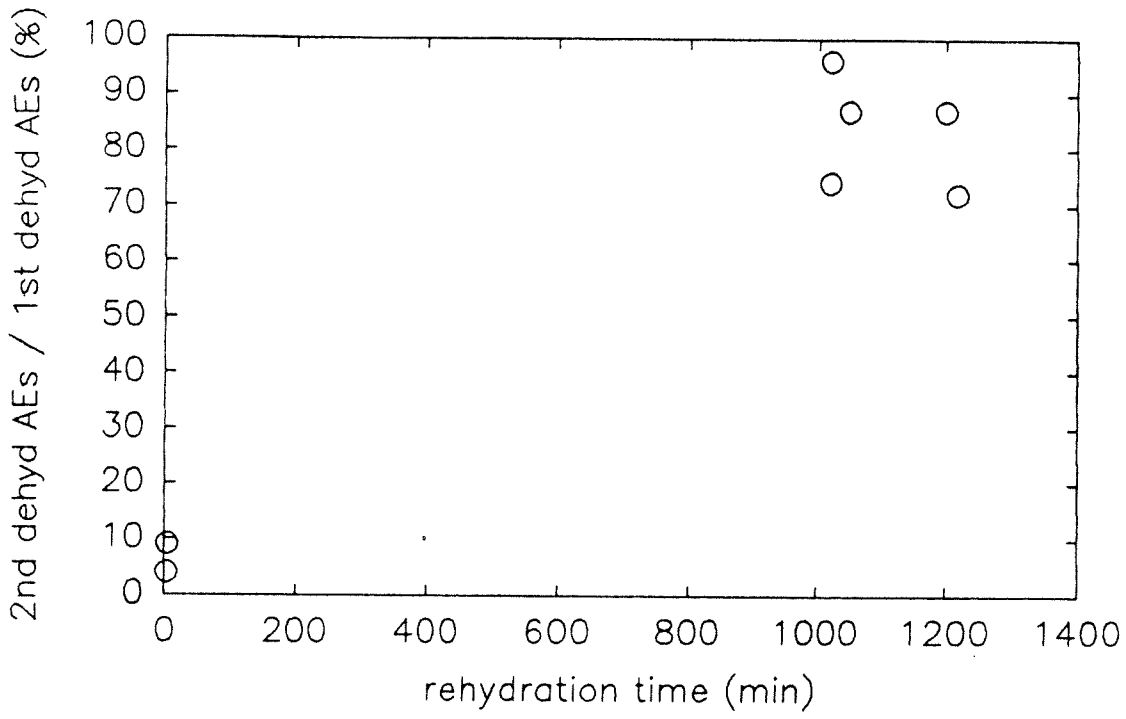
2nd dehyd AEs / 1st dehyd AEs (%)
100
90
80
70
60
50
40
30
20
10
0
0
200
400
600
800
1000
1200
1400
rehydration time (min)

Fig. 3.5. AEs detected during dehydration of a longitudinal section. Occurrence of events detected visually during dehydration are superimposed with an event marker on a chart recorder. 1) Menisci form at cuts in tracheids at the section's surface and begin to move through these cut tracheids. 2) Menisci move slowly through tracheids on the surface, and more rapidly through somewhat more deeply embedded tracheids. 3) Menisci move even more rapily through more deeply embedded tracheids. A few deep tracheids rapidly change from translucent to opaque. 4) Rapid transparency changes increase in frequency. Very few slow movements of menisci visible; most of these are in deep layers. 5) Dramatic increase in number of rapid transparency changes in deep tissue layers. A few slow movements of menisci in deep tissue layers. Some gross tissue movement occurs towards the end of this time period. 6) End of all visible activity. Figure events 4 and 5 occur within the third stage of dehydration as described in the text. Gross tissue movement is the text's Stage 4, and Stage 5 corresponds to Event 6 in this figure.

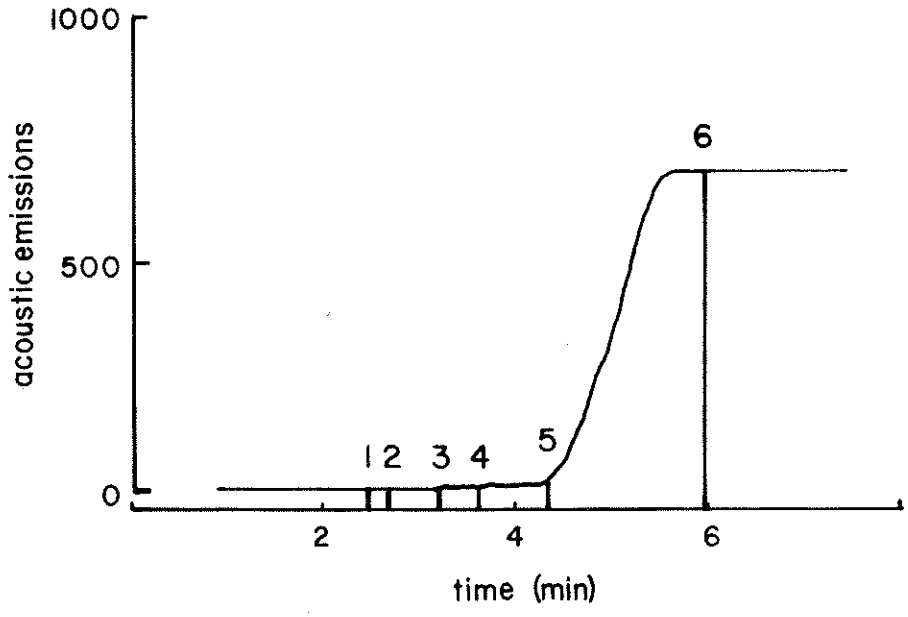
1000
500
0
acoustic emissions
1 2 3 4 5 6
2
4
6
time (min)

CHAPTER 4

Embolism in Fully Hydrated *Thuja occidentalis* Tracheids Under Water Stress is Caused by Air-seeding[1]

INTRODUCTION

As outlined by Zimmermann (1983), air-seeding in a xylem sap-filled fiber, tracheid, or vessel should occur when the lumen pressure potential (Ψ_p) falls below a threshold described by the capillary equation (Chap. 2). When Ψ_p reaches this threshold, external air enters the lumen through the largest pore or crack in the cell wall which is in contact with the air (Fig. 4.1). One could easily imagine this process occurring in gymnosperms which have pores in the pit membranes. The membrane structure was described as early as 1916 by Bailey who suggested that the valve-like action of the membranes prevented air from moving from tracheid to tracheid through the pores. He measured pore diameters by particle infiltration, and found that the pores were large enough to admit air at the tensions predicted by the tension hypothesis for the ascent of sap. Eicke (1958) described the pit membrane pores in several gymnosperm families using light microscopy. The idea of embolus formation by air-seeding did not gain

[1] This chapter will be submitted in modified form to the International Association of Wood Anatomists Bulletin for publication.

wide acceptance in part because perforated pit membranes could not be found in angiosperms even when EM techniques were used. Bonner and Thomas (1972) and Meylan and Butterfield (1982) were among the first to prepare angiosperm samples which had visible pit membrane pores. It seems that sample preparation methods allowed coating of the microfibrils by plant wound substances which prevented previous imaging of the perforations. Now that structure is known to be consistent with theory, and now that cavitation can be detected and plant water potential can be measured, we can confirm the air-seeding hypothesis.

In an undamaged *Thuja occidentalis* tracheid, the largest hole in the cell wall is a pore in one of the pit membranes. If an adjoining tracheid contains air at a sufficiently higher pressure than the sap-filled tracheid, air will be forced into the sap-filled tracheid lumen through a connecting pore, in the form of a bubble. As quickly as the lumen tension is relieved by bubble entry, some of the lumen sap evaporates into the bubble, and some is released to surrounding tissue (Chap. 3). The bubble expands to fill the lumen. The exact dynamics of the bubble are not known. It is not clear that the bubble actually pulls free from the pore immediately as shown in Figure 1.1 of this thesis and in Figure 3.6 of Zimmermann (1983); the bubble does not pull free from the pore in *Sphagnum* hyalocysts (Chap. 2).

The data presented here were obtained primarily from pressure bomb and countertop dehydrations. The data show that fully hydrated *Thuja occidentalis* tracheids embolize by air-seeding when exposed to water stress. Differences in dehydration by water stress and by positive pressure in a pressure bomb are discussed with respect to cavitation and air-seeding. Additionally, the significance of the pattern of

embolized tracheids in the xylem will be related to our understanding of embolism.

MATERIALS AND METHODS

Plant Material. All experiments were conducted using stem wood from *Thuja occidentalis* L. orthotropic shoots. The excised shoots were rehydrated for a minimum of 8 to 10 hours using the method described in Chapter 3. Hydrated stems were cut into segments 10 cm in length under tap water filtered to 0.7 μm and degassed to approximately -0.1 MPa. Shoots for the "simulated air-seeding" experiments were collected from an overgrown plantation at the Harvard Forest, Petersham MA. The shoots resulted from ground layering of fallen trees. Saplings for other experiments were greenhouse grown. Samples for experiments were taken from wood that was 9 or fewer years old.

Simulated Air-seeding. Stem segments were dehydrated by positive pressure in a pressure bomb in order to simulate the pressure differential across cell walls to which tracheids are exposed under water stress. Two types of experiments were conducted under these conditions. In each, the hydrated segment was debarked, patted dry with towelling, weighed, and inserted in the pressure bomb with approximately 1 cm of the apical portion exposed on the exterior of the bomb. A very wet sponge was placed in the bomb to maximize the relative humidity of the gas which was forced through the segments, in order to minimize evaporative drying of the tissue. A glass vial, containing a tight roll of filter paper, was placed upside down on the

exposed stem so that the top of the stem touched the paper (Fig. 4.2). The vial was capped and weighed at intervals during each step of the dehydration. Bomb pressure was raised in a series of steps. At each step, the pressure was held constant until all visible water stopped exuding from the exposed stem surface and the weight of the vial stopped increasing (usually 5 to 10 min). Maximum vial weight was recorded for each bomb pressure increment.

In one set of experiments, for each of several segments, the pressure was raised in 0.2 MPa increments until it reached at least 4.0 MPa above ambient pressure. The segment was removed from the pressure bomb after releasing the pressure, weighed, oven dried at 70°C overnight, and reweighed. Weight of expressed water was plotted against bomb pressure as a means of describing the amount of water lost compared to the applied pressure.

In the other set of pressure bomb experiments, each segment was raised to a predetermined pressure by 0.2 MPa increments as described above. When water exudation at that pressure stopped, the bomb pressure was released and the segment was removed from the bomb, weighed, wrapped in plastic wrap, and placed in the dark. Following a one-half hour equilibration, dye was pulled through the segment, as described below, to mark conducting (non-embolized) tracheids.

Countertop Dehydrations. Ideally, the above experiments would have been performed by dehydrating the segments by evaporation on the countertop at ambient pressure. Ψ_p would then have been determined by obtaining a balance pressure in the pressure bomb (-balance pressure = $\Psi \tilde{=} \Psi_p$, where Ψ is plant water potential). Unfortunately, it was not possible to obtain balance pressures on

T. occidentalis stem segments, presumably because there is too little parenchymatous tissue to act as a water reservoir. The pressure bomb dehydrations were selected as an efficient alternative.

Pressure bomb dehydrations may differ from dehydrations which proceed under tension in two ways. The first difference is addressed in Chapter 3: ultrasonic acoustic emissions are not produced, so that the process of bubble entry may not be as energetic when driven by the application of positive pressure. However, the pressure differential is the same, and, assuming that emboli are formed in both cases by bubbles pulling through the same pores, similar results should be obtained if bomb dehydrations are conducted to the point of "stability" at the final pressure as described. Differences may result also if the applied pressure causes gas to dissolve in the lumen sap which then comes out of solution during or after the release of bomb pressure. The process may be similar to that of nitrogen evolving from the blood of human divers who stay submerged for long periods without decompression upon ascent. The pattern of distribution of tracheids with emboli formed by "the bends" could be very different from the pattern created by air-seeding. Countertop dehydrations of stem segments were conducted to control for this possibility.

Ten-cm-long hydrated segments were countertop dried to predetermined fractions of their wet weight. These fractions were chosen to be within the same range as those from the pressure bomb dehydrations. The dehydrated samples were wrapped in plastic wrap and placed in the dark for one-half hour. After the equilibration time, dye ascents were conducted in the same manner as in the pressure bomb dehydrated segments.

Dye Ascents. Each 10-cm-long segment was reweighed after the equilibration time elapsed. Weights decreased little (less than 0.5%), if at all, during this time. Both ends were trimmed under 5 mM KCl which was filtered to 0.45 μm and degassed under vacuum to approximately -0.100 MPa. Final cuts were made with a sharp razor blade. Basic fuchsin (0.2% w/v) in 5 mM KCl (filtered to 0.45 μm and degassed under vacuum to approximately -0.100 MPa) was pulled through the segment by placing the basal end of the 5-cm segment in a 1-cm-deep dye bath and applying -0.084 vacuum to the apical end for 4 min (Fig. 4.3). By closing the stopcock, the vacuum could be reduced without completely releasing it. The basal end of the segment was transferred quickly to a 2-cm-deep bath of 5 mM KCl. The KCl was pulled through the segment for an additional 8 min by reopening the stopcock. This transfer method prevents air emboli from entering the basal cut tracheids, yet restricts dye movement into partially embolized tracheids. After removing the KCl bath, the vacuum application at the apical end continued for another 3 min to draw out excess water. The segments were left on the countertop to dry for 0.5 to 1.5 hours before sectioning. Several trials proved that this protocol infused satisfactory quantities of dye even in some of the driest segments without leaving enough excess to create smearing problems during sectioning.

Sections, 45 μm thick, were taken from the apical end of the segment after removing enough material to get a full transverse section and from the base after removing just over 1 mm of the base to remove the tracheids which had been cut and exposed to the dye bath. An additional section was taken from the center of the segment.

Microscopic observation of test material indicated that the most consistent dye patterns were obtained in the apical section.

In order to obtain quantitative data, two radial rows of tracheids were selected from the apical section of each sample. These rows approximately opposed each other across the pith. Each tracheid from the selected rows was scored for dye content in the cell wall and lumen diameter along the segment's radius was measured. Tracheids with dye stained walls were interpreted as conducting and having no emboli. Diameter was recorded in 2 μm diameter classes; the tally was kept by growth ring. All growth rings except the most recent were counted. Counts in the outermost ring would have been skewed by damage in that ring from debarking and by immature tracheids near the cambium.

Pit Membrane Pore Diameter. Estimates of the largest pore diameters in tracheid-to-tracheid pit membranes were made by passing india ink and paint pigments through 5-mm-long, fully hydrated stem segments. Higgins Waterproof India Ink and brown iron oxide Universal paint pigment (diluted approximately 1:10, v/v, with distilled deionized water) were filtered with Millipore 5.0 μm SM, 0.45 μm HA, and 0.22 μm GS filters in stages. Each of the suspensions that passed through the 0.22 and 0.45 μm filters were dripped through stem segments by gravity feed, with a hydrostatic pressure head of about 1.5 cm. The filtrate was collected on chromatography paper. Chromatography paper was colored by the filtrate if the particles could pass through the segment. Diameters of the passed particles were checked with SEM.

Direct measurement of large pore diameters was attempted using SEM. Material was fixed in glutaraldehyde, rinsed in several changes of phosphate buffer, and dehydrated in alcohol series, before critical

point drying, cutting with a new razor blade, and sputter-coating with Au-Pd (a process similar to that of Meylan and Butterfield, 1982). The samples were examined by SEM at 68,000X.

RESULTS

Susceptibility to Embolism of Larger versus Smaller Tracheids. As a general rule, the largest diameter xylem conduits are also the longest conduits (i.e., vessels are both longer and wider than tracheids and wide vessels are usually longer than narrow vessels). In the past, the largest xylem conduits, those with the greatest volume, were thought to be more prone to developing emboli than the smallest conduits (e.g., Ewers, 1985; Tyree et al., 1984b; Tyree and Dixon, 1986, and literature cited therein), because the largest cells have the greatest sap volume and the greatest wall area. Random events which may lead to cavitation and embolism should have the greatest chance of occurring within the largest sap volumes (Oertli, 1971). Likewise, those cells with the greatest cell wall surface should be more likely to have wall surface imperfections that could trigger cavitation (Tyree and Dixon, 1986). In their investigations on embolism induced by water stress in *T. occidentalis*, *Tsuga canadensis*, and *Acer saccharum*, Tyree and Dixon (1986) gathered data that indicated that *Acer* vessels embolized at lower water potentials than did either *Thuja* or *Tsuga* tracheids. Since *Acer* vessels are larger (longer and wider) than *Thuja* or *Tsuga* tracheids, the generalization does not necessarily hold between species. Within each species, the percentage of water lost per

acoustic emission (AE) decreased as dehydration progressed, indicating that the larger conduits within a species do develop emboli before the smaller ones.

Careful examination of the dye ascent data from the experiments reported herein shows that within a stem segment, tracheid location rather than tracheid size determines when a tracheid embolizes. In the pressure bomb dehydrations (countertop dehydration results are similar), large diameter tracheids usually develop emboli at lower bomb pressure, or higher Ψ_p, than smaller diameter tracheids. But it is clear that some large diameter tracheids embolize after some small diameter tracheids (Figs. 4.4 and 4.5). In this histogram and those following, the open bars indicate conducting or stained tracheids; the closed bars indicate non-conducting or unstained tracheids. In these experiments, earlywood tracheids developed emboli before (at lower bomb pressure or higher Ψ_p) latewood tracheids regardless of diameter. The first few layers of earlywood tracheids frequently had smaller radial diameters than tracheids which developed later in the growing season, even though the largest diameter tracheids were usually in earlywood.

The data from growth ring 2 of four specimens subjected to different bomb pressures show the tendency for larger tracheids to embolize first (at lower bomb pressure or higher Ψ_p) (Fig. 4.5). Rings are numbered from the inside outwards, so that the first year's growth of a shoot is ring 1. At a bomb pressure of 0 MPa, all tracheids conduct. At 1.2 MPa many of the larger tracheids are embolized. With increasing bomb pressure, smaller and smaller tracheids embolize and few large tracheids continue conducting. At high bomb pressure, or low Ψ_p, small tracheids are the major conductors.

It is evident that this is not a strict rule. We have recorded instances in which the largest tracheids continued to conduct while the smallest embolized. In these cases, bomb pressures of 3.0 and 4.0 MPa, some of the smallest tracheids developed emboli while much larger ones conducted dye. The equivalent Ψ_ps (-3.0 and -4.0 MPa) are lower than have been recorded in the field for this species. Usually, when the smallest tracheids are non-conducting while earlierwood tracheids in the same ring conduct, the small tracheids abut non-conducting ones in the earlywood of the next growth ring. This supports the idea that embolism is passed from conduit to conduit. Isolated non-conducting tracheids are rarely found. The picture is also complicated by the tendency for the inner growth rings to embolize at lower bomb pressures, higher Ψ_ps, than the outer rings (Fig. 4.6). In this segment, which was pressurized to 1.2 MPa, ring 1 is almost entirely embolized, while ring 2 has only a few tracheids containing emboli, and all tracheids in rings 3 and 4 are transporting. The trend toward the production of larger tracheids in the outer rings is also apparent here, where the average tracheid diameter increases from ring 1 to ring 4.

At high bomb pressure (e.g., 4.0 MPa), or low Ψ_p, the majority of tracheids, especially the larger ones, are embolized, so that the ratio of the average diameter of conducting tracheids to the average diameter of all tracheids in a sample is relatively small (Fig. 4.7). At low bomb pressure (e.g., 1.0 MPa), or high Ψ_p, the tendency for earlywood tracheids (i.e., generally, the larger tracheids) to embolize first is balanced by the tendency for inner rings (i.e., rings with smaller average tracheid diameters) to embolize first, so that the ratio is

close to one.

Pore Diameters. SEMicrographs show pores in a pit membrane that are very elongate, with the largest effective pore diameter (the short dimension) of just over 0.1 μm (Fig. 4.8). The membrane in the figure may be aspirated. The pit is encrusted and may be coated with something other than Au-Pd. The sample preparation was poor, and very few intact, uncoated membranes could be found. Other pit membranes appear to be smoothly coated with what may be wound reaction substances. Some samples had pit membranes that were filamentous, as expected, but none were intact. If the pictured membrane is indeed encrusted, the coating could have decreased the pore diameters to less than one-half of their original values. In their SEM investigations of pit membranes Bauch et al. (1972) provided photographs of *T. occidentalis*. The largest pits have long axes on the order of 0.3 μm, assuming that the pores are measured in a manner consistent with the discussion on pore diameter in Chapter 2 (i.e., the pores are assumed to be circular, elliptical, or retangular). The pores in their pictured membrane are roughly circular or elliptical.

Brown iron oxide filtrate with the largest particle diameters measuring 0.45 μm did not pass through stem segments. Brown iron oxide filtered to remove particles greater than 0.22 μm passed easily through a segment and stained the chromatography paper. SEM photographs of the unfiltered pigment show that the smallest pigment particles have diameters of approximately 0.10 μm and the largest have diameters of 0.30 μm. The 0.45 μm filter probably passed some clumped particles of which the unfiltered pigment was primarily composed. These are likely to block the pit membrane pores, effectively preventing the passage of

smaller particles. SEM examination showed that particles as large as 0.22 μm passed through a stem segment and deposited on the chromatography paper (Fig. 4.9A). These particles were from the 0.22 μm filtrate and were spherical.

India ink particles have a much broader diameter distribution than do the particles of brown iron oxide. The filtrate from the 0.22 μm filter passed easily through a stem segment, leaving the paper darkly colored. Filtrate from the 0.45 μm filter did not initially color the chromatography paper, and the liquid from the suspension took significantly longer to drain from the reservoir. After this liquid had completely drained, a small spot of color was found on the paper. We assume that some of the smallest diameter particles were able to bypass blocks caused by larger particles. SEM examination showed that particles as large as 0.21 μm from the 0.22 μm filtrate deposited on the chromatography paper after passing through a stem segment (Fig. 4.9B). The smallest particles detectable against the background of the chromatography paper were on the order of 0.04 μm in diameter. India ink particles are only roughly spherical in shape.

An attempt to pass 0.08 μm monodispersed polystyrene beads (Polysciences, Inc., Warrington PA) through stem segments was remarkably unsuccessful. SEM examination showed that a few beads did pass through the membranes, but most of the beads were clumped in the pits near the end to which they were applied. Surface charges on the beads probably interact with the pit membrane and prevent passage of the beads (Fig. 4.10).

Air-seeding. Figure 4.11 presents typical curves representing the weight of water expressed from stem segments at various bomb pressures

for the pressure bomb dehydrations. The threshold pressure at which the slope changes rapidly (indicating rapid water loss) varies with each sample, but falls between 0.8 and 1.8 MPa in all samples, and most commonly is between 0.9 and 1.1 MPa. Bubbling from the tracheids is first detectable in the vicinity of the threshold pressure for a given sample. The first non-conducting tracheids appear in dye ascents made after pressurization of a segment to the threshold pressure for that particular sample. The threshold pressure varies from sample to sample but its range is restricted. When several curves are combined to average them, as in Tyree and Dixon (1986), the abruptness of the change in slope for a particular specimen is obscured. Analysis of dye ascent data from several samples indicates that the percentage of stained tracheids decreases sharply in the same pressure range, as does the calculated hydraulic conductivity (Fig. 4.12). Tyree (personal communication) monitored Ψ_p for *T. occidentalis* in the field during a dry summer north of Toronto, Ontario. The lowest Ψ_p that he measured was approximately -1.5 to -1.8 MPa.

Countertop dehydrations are used to control for the possibility of skewed results from the evolution of dissolved gases after pressure release in pressure bomb dehydrations. The final weight after dehydration as a percentage of the fully hydrated (wet) weight is used as a parameter to relate pressure bomb and countertop dehydrations to each other. In Figure 4.13A, the greatest decrease in the percentage of stained tracheids occurs at 80 to 90% of wet weight for pressure bomb dehydrations. For countertop dehydrations, that decrease occurs between 75 and 80% (Fig. 4.13B). 80% of wet weight is the equivalent of a bomb pressure approximately equal to 2.0 MPa (Fig. 4.14). If the

discrepancy is the result of the bends, the water forced out by the release of gases from solution at the onset of embolism accounts for just over 5% of the wet weight. The difference is probably within the limits of individual variation. The countertop dehydrations show that any gases which may come out of solution upon depressurization of pressure bomb dehydrations do not dramatically affect the number of stained tracheids. It is interesting to note that Tyree and Dixon (1983) detected the beginning of embolism during both air (countertop) and pressure bomb dehydration of *T. occidentalis* at a pressure differential of approximately -1.0 MPa using ultrasonic acoustic emissions as an indicator. Ψ_p was estimated for the countertop dehydrated shoots by the determination of balance pressure for excised subsamples. The specimens themselves were not subjected to elevated pressures. Under these conditions, their results show no evidence for the bends. For the experiments reported in this thesis, the bends should not create large discrepancies within the pressure ranges of concern, i.e., bomb pressures of 1.0 to 2.0 MPa.

DISCUSSION

Susceptibility to Embolism of Larger versus Smaller Tracheids. The data reported for stem segments may differ from that which would be obtained from whole shoots. In stem segments, the pith is exposed at both ends and provides a low resistance pathway for water and air movement. Air usually penetrated the pith at approximately 1.0 MPa bomb pressure, as evidenced by bubbling from the pith. It is not known

whether the pith empties of water at Ψ_p = -1.0 MPa in the intact plant. Sperry, Donnelly, and Tyree (personal communication) found that shoots of *Acer saccharum* dehydrate with a different pattern of embolism than do stem segments. They attribute the differences to the continuity of exposed pith in the stem segments.

Several other errors may influence the results that are reported here. The negative of the bomb pressure at which the segments were dehydrated is taken as the water potential of the segment after dehydration. If the osmotic potential of lumen water is close to zero, then $\Psi = \Psi_p$. Using -bomb pressure = Ψ may not be accurate because the water loss through evaporation into the perfusing gas in pressure bomb dehydrations is difficult to quantify (i.e., the bomb pressure at the end of the dehydration may not be a true balance pressure). Evaporation of water from the filter paper during pressure bomb dehydrations can create errors by reducing the amount of expressed water weighed (see Fig. 4.2). Fortunately, errors resulting from either the exposed pith or airways through the tracheids should be significant only once large volumes of gas escape through the tissue. Water vapor cannot escape in quantity with the perfused gas until the passages are empty of water, that is, at high bomb pressures. The pressures of most importance in this work are those in the lower ranges, those at which both the tracheids and the pith are just begining to open to gas flow.

Since both the water potential at which embolism occurs and rate of refilling are components of a tracheid's susceptibility to embolism, the possibility of refilled tracheids further complicates the interpretation of our results. Embolized conduits can refill when

dehydrated under tension (Chap. 3). Conduits that contain water vapor refill as soon as the pressure is increased. Small air-filled conduits may refill with water quickly after the tension is released and replenishment water is available. Larger conduits may not be able to refill when they contain air, or they may take more time and/or may require high Ψ_ps to refill. On the other hand, it is unlikely that tracheids which embolize at high pressure, as in the pressure bomb dehydrations, will refill when the pressure is reduced. It is much more likely that any bubbles introduced into tracheid lumens at high pressure will continue to expand if the pressure is reduced. None-the-less, it is important not to consider our results as descriptive of plants in their habitats, or even of intact plants. The dye ascent data are primarily intended to be interpreted qualitatively and as indicators for directions in which further investigations should proceed. The extension of quantitative conclusions to intact plants and to plants in the field must be delayed until further correlation between excised laboratory material and whole plants is obtained.

Pore Diameters. Although the particle perfusions are consistent with each other, obtaining direct evidence of the pit membrane pore diameters and of membrane condition during embolus production is a top priority for continuing work. The pores are too small to be clearly distinguished under a light microscope with green or blue light, therefore they must be on the order of, or less than, 0.25 to 0.30 μm in diameter. Evidence of the thickened torus is visible under the light microscope. If *T. occidentalis* pore diameters prove too elusive, *T. plicata* may be better suited to the study. No evidence of a thickened central area on the pit membrane is evident under the

microscope, and its larger pores may be more easily documented. Liese and Bauch (1964) measured pore diameters by TiO_2 infusion of 0.125 to 0.182 μm for *T. plicata* and 0.110 to 0.165 μm for *T. occidentalis*. We still have no good evidence to indicate how drying and fixation methods for EM affect the measured pore dimeters. Most of the more recent pore diameter measurements come from the wood technology literature where the primary concern is the passage of preservatives into the wood (Siau, 1984, and literature cited therein). The wood technologists are primarily concerned with the diameters of those pores which pass the majority of fluid and not necessarily the maximum pore diameters. Other authors (Carpita, 1982; Van Alfen et al., 1983) report plant cell wall pore diameter measurements, but none that are of use here.

The pressure differential (MPa) required to pull an air-water interface through a pore of diameter D (μm) to air-seed the cell is given by $\Delta P \tilde{=} 0.3/D$ (Chap. 2). If the largest pore diameter is 0.1 μm, then $\Delta P = 3.0$ MPa (i.e., $\Psi_p = -3.0$ MPa; and for pressure bomb dehydrations, bomb pressure = $\Delta P \tilde{=} -\Psi_p = 3.0$ MPa), a value more extreme than that recorded in *T. occidentalis*. On the other hand, if $D = 0.2$ μm, from the particle infusion measurements in our lab, $\Delta P = 1.5$ MPa. Using the pore diameter measurement from the photograph of Bauch et al. (1972), $D = 0.3$ μm gives a value for ΔP of 1.0 MPa. Both of these values are consistent with data gathered in this study in support of the air-seeding hypothesis. Bauch et al. also show a latewood pit membrane with typically smaller perforations. The largest of these are on the order of 0.1 μm, which would indicate that the latewood should embolize at a $\Psi_p = -3.0$ MPa. The results of this study are consistent with the reported pore diameter for latewood.

Figure 4.12A shows that about 20% of the tracheids in a sample are functional at Ψ_p = -3.0 MPa (3.0 MPa bomb pressure), the number of conducting tracheids falls to less than 10% at Ψ_p = -4.0 MPa (4.0 MPa bomb pressure).

Ideally, lumen pressure measurements should be correlated with maximum pore diameters for individual tracheids. Lacking the ability to work with individual tracheids, we should be able to statistically correlate pore diameters with Ψ_p at embolism in latewood and earlywood. With careful preparation methods, pore diameter measurements from specific areas of tissue should be obtainable. The technology now exists to measure Ψ_p at embolism with stem psychrometers and to determine the embolized tissue with dye ascents.

Air-seeding. Our understanding of the evolution of dissolved gases after a release of pressure is incomplete. As confirmed by divers who suffer from the bends, the theory of bubble generation from gases dissolved at elevated pressure predicts a much higher threshold pressure for the evolution of nitrogen than is the reality (Pickard, 1981). Experimentally, Tyree et al. (1984a) found discrepancies in Ψ_p at the start of acoustic emission accumulation between pressure bomb dehydrations and air dehydrations. They attribute this to the bends. Their bomb dehydrated samples were raised to a high pressure (2.0 to 2.5 MPa) and left for several hours at that pressure. In their air dehydrations, balance pressures were taken on the samples. Since the the samples were pressurized only long enough to obtain a balance pressure at each measurement, the air dehydrations are less likely to be affected by gases dissolved at high pressures. Exposing xylem water to high pressures for extended periods is much more likely to dissolve

gases than the method which we employed. Sperry (personal communication) observed bubbles emanating from the cut surfaces of *Rhapis* stem and petiole segments. The segments had been pressured in a bomb, then submerged in water for rehydration. He suggests that bubble production under these circumstances indicates that the bends occurs in pressure bomb dehydrations of stems. We noticed the evolution of bubbles in *Thuja* stem segments that were partially dehydrated under pressure and put in water. These bubbles may be gas that is released from solution. Alternatively, they may be gas that was forced into tracheid lumens under pressure which expands after the pressure is released and gradually makes its way towards the cut surfaces through the network of air-filled tracheids. It is reasonable to expect gas release due to this expansion for a short time after depressurization, so that Sperry's bubbles may not be evidence of the bends.[2]

Both countertop and pressure bomb dehydrations produce non-conducting tracheids. Both do so by the production of emboli, gas bubbles that are large enough to block the flow of sap through conduits. In both types of dehydration, a gas bubble can be initiated in a tracheid by air entering the lumen through a pore in the pit membrane. The formation of this type of embolus is driven by the pressure differential (ΔP) between the tracheid lumen and the exterior. The pressure differential creates a pressure drop across the air-water interface near the cell wall and pushes the meniscus through the pore in the form of a bubble. In countertop dehydrations (drying by

---

[2] Current plans are to repeat both countertop and pressure bomb dehydrations on uniform specimens, and to use a stem psychrometer to directly measure Ψ_p.This comparison should give additional insight into the the enigma of the bends. The stem psychrometer was not available for the current study.

evaporation which creates tension, in this case $\Psi_p \leq -0.8$ MPa), an ultrasonic AE is produced for each embolus which develops in this way. Production of an ultrasonic AE indicates an energetic event, which is a cavitation (Chap. 3). Since no ultrasonic AEs are detected when *T. occidentalis* tracheids develop emboli by dehydration under positive pressure in a pressure bomb, we conclude that cavitations are not produced under these circumstances. Even though the process is not energetic, and cavitations are not produced, the capillary equation does describe the behavior of the meniscus. We may call this air-seeding, although not quite in the same sense that Zimmermann (1983) conceived of air-seeding.

In summary, an embolus formed by air-seeding under tension may initially be composed primarily of water vapor. Tyree and Dixon (1986) suggest that it may take hours for enough air to diffuse through to the interior of water stressed tissue to significantly alter the composition of bubbles in the innermost growth rings. If tissue containing water-vapor emboli is rehydrated, these emboli will collapse immediately, leaving the tissue unblocked by bubbles. On the other hand, emboli containing high fractions of air may shrink but continue to occupy enough lumen volume to effectively slow or stop transport. An embolus formed by air-seeding under positive pressure in a pressure bomb is likely to be composed mostly of air. Application of positive pressure during pressure bomb dehydration may dissolve gases which come out of solution when the tissue is returned to atmospheric pressure. Pressure bomb dehydrations should not give rise to emboli formed by expansion of entrapped bubbles, as countertop dehydrations do. In fact, bubbles entrapped at atmospheric pressure or below may collapse

when exposed to the pressure increase inherent in bomb dehydrations. Clearly, we must be cautious when using pressure bomb dehydrations to reach conclusions about the effects of air dehydration; the two processes are not the same and do not necessarily yield the same results.

LITERATURE CITED

Bailey IW 1916 The structure of the bordered pits of conifers and its bearing upon the tension hypothesis of the ascent of sap in plants. Bot Gaz 62: 133-142, 1 plate

Bauch J, W Liese, R Schultze 1972 The morphological variability of the bordered pit membranes in gymnosperms. Wood Sci Technol 6: 165-184

Bonner LD, RJ Thomas 1972 The ultrastructure of intercellular passageways in vessels of yellow poplar (*Liriodendron tulipifera*, L.), part I: vessel pitting. Wood Sci Technol 6: 196-203

Carpita NC 1982 Limiting diameters of pores and the surface structure of plant cell walls. Science 218: 813-814

Eicke R 1958 Die Bedeutung der Feinstruktur der Hoftüpfel für die Phylogenie der Gymnospermen. Z Botanik 46: 5-15

Ewers FW 1985 Xylem structure and water conduction in conifer trees, dicot trees, and lianas. IAWA Bull ns6: 309-317

Liese W, J Bauch 1964 Über die Wegsamkeit der Hoftüpfel von Coniferen. Naturwisseschaften 21: 516

Meylan BA, BG Butterfield 1982 Pit membrane structure in the vessel-less woods of *Pseudowintera dandy* (Winteraceae). IAWA Bull ns3: 167-175

Oertli JJ 1971 The stability of water under tension in the xylem. Z Pflanzenphysiol 65: 195-209

Pickard WF 1981 The ascent of sap in plants. Prog Biophys molec Biol 37: 181-229

Siau JF 1984 Transport Processes in Wood. Springer-Verlag, Berlin, Heidelberg, New York, Tokyo

Tyree MT, MA Dixon 1983 Cavitation Events in *Thuja occidentalis* L.?: ultrasonic acoustic emissions from the sapwood can be measured. Plant Physiol 72: 1094-1099

Tyree MT, MA Dixon 1986 Water stress induced cavitation and embolism in some woody plants. Physiol Plant 66: 397-405

Tyree MT, MA Dixon, RG Thompson 1984a Ultrasonic acoustic emissions from the sapwood of *Thuja occidentalis* measured inside a pressure bomb. Plant Physiol 74: 1046-1049

Tyree MT, MA Dixon, EL Tyree, R Johnson 1984b Ultrasonic acoustic emissions from the sapwood of cedar and hemlock: an examination of three hypotheses regarding cavitations. Plant Physiol 75: 988-992

Van Alfen NK, BD McMillan, V Turner, WM Hess 1983 Role of pit membranes in macromolecule-induced wilt of plants. Plant Physiol 73: 1020-1023

Zimmermann MH 1983 Xylem Structure and the Ascent of Sap. Springer-Verlag, Berlin, Heidelberg, New York, Tokyo

Fig. 4.1. During air-seeding, a meniscus should enter a tracheid lumen through the largest hole in the tracheid wall which is in contact with external air. A, Diagram showing a typical conifer bordered pit membrane with the torus, a thickened area of the membrane, and the margo which is perforated. The arrow indicates the largest pore in the margo. In undamaged tracheids, a pore in the pit membrane should be the largest diameter opening in the cell wall. B, Diagram depicting an air-seed entering a tracheid lumen at a bordered pit which is in contact with an embolized tracheid.

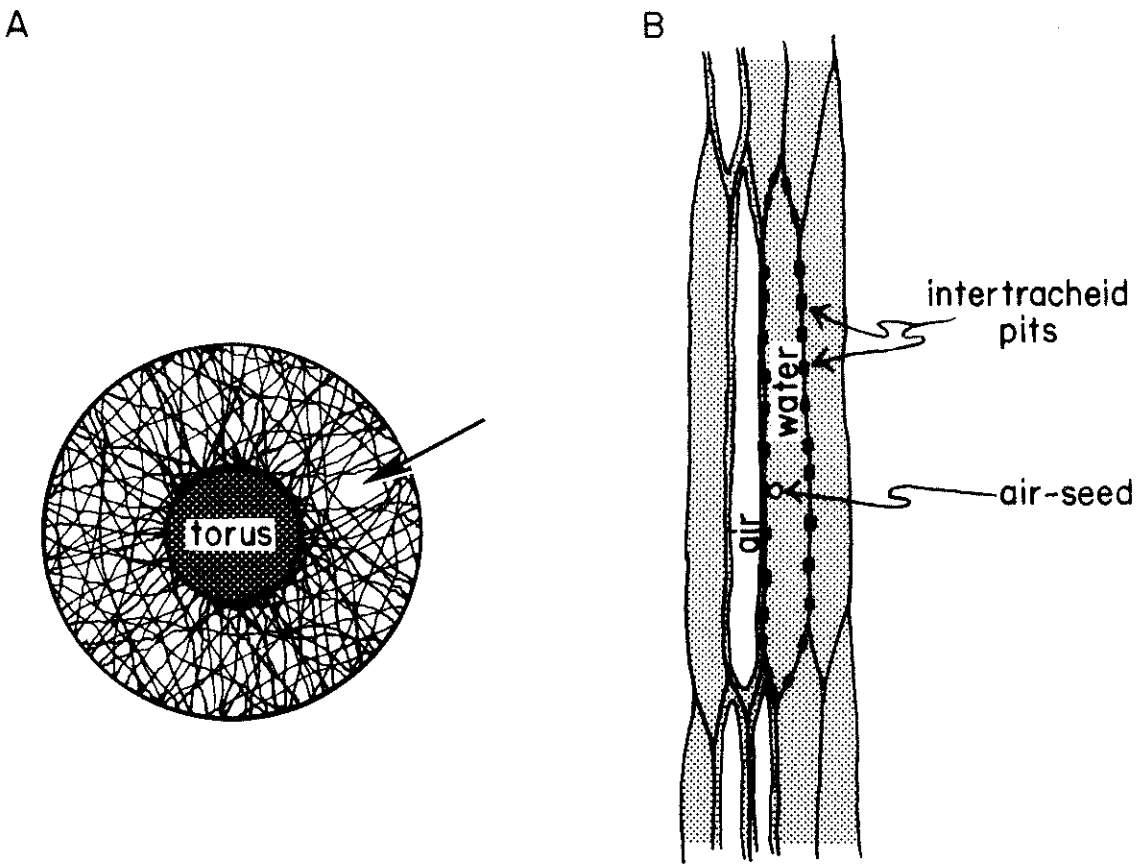
A
torus
B
intertracheid pits
water
air
air-seed

Fig. 4.2. Diagram of a stem segment in a pressure bomb. The vial containing filter paper is inverted over the stem segment to collect expressed water when the bomb is pressurized. The vial is capped and weighed at intervals to determine the amount of water released at various bomb pressures.

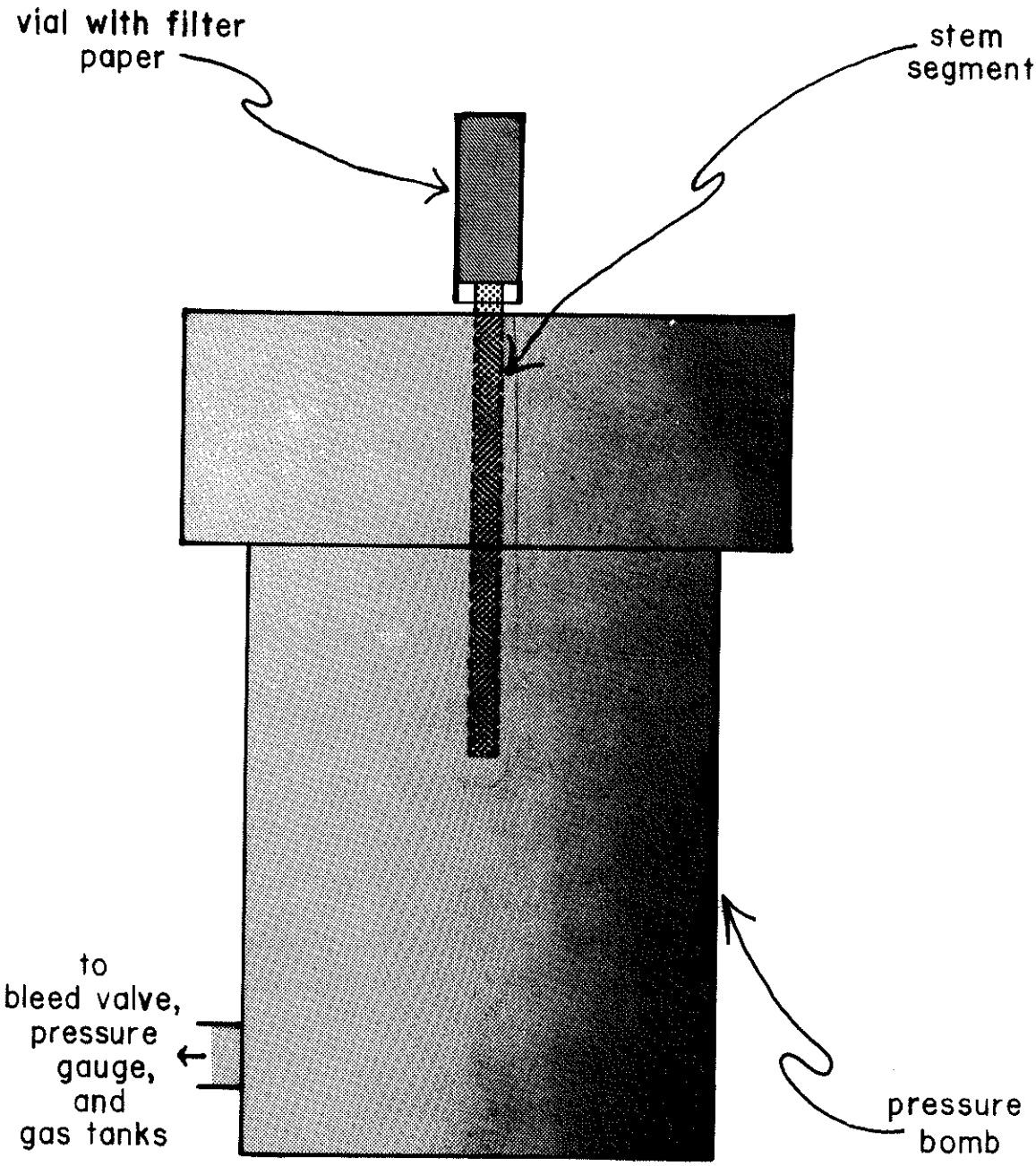
vial with filter paper
stem segment
to bleed valve, pressure gauge, and gas tanks
pressure bomb

Fig. 4.3. Dye ascent apparatus. Dye is drawn through the stem segment by vacuum. Closing the stopcock allows a water bath to be substituted for the dye bath without completely releasing the vacuum and without maintaining a full vacuum.

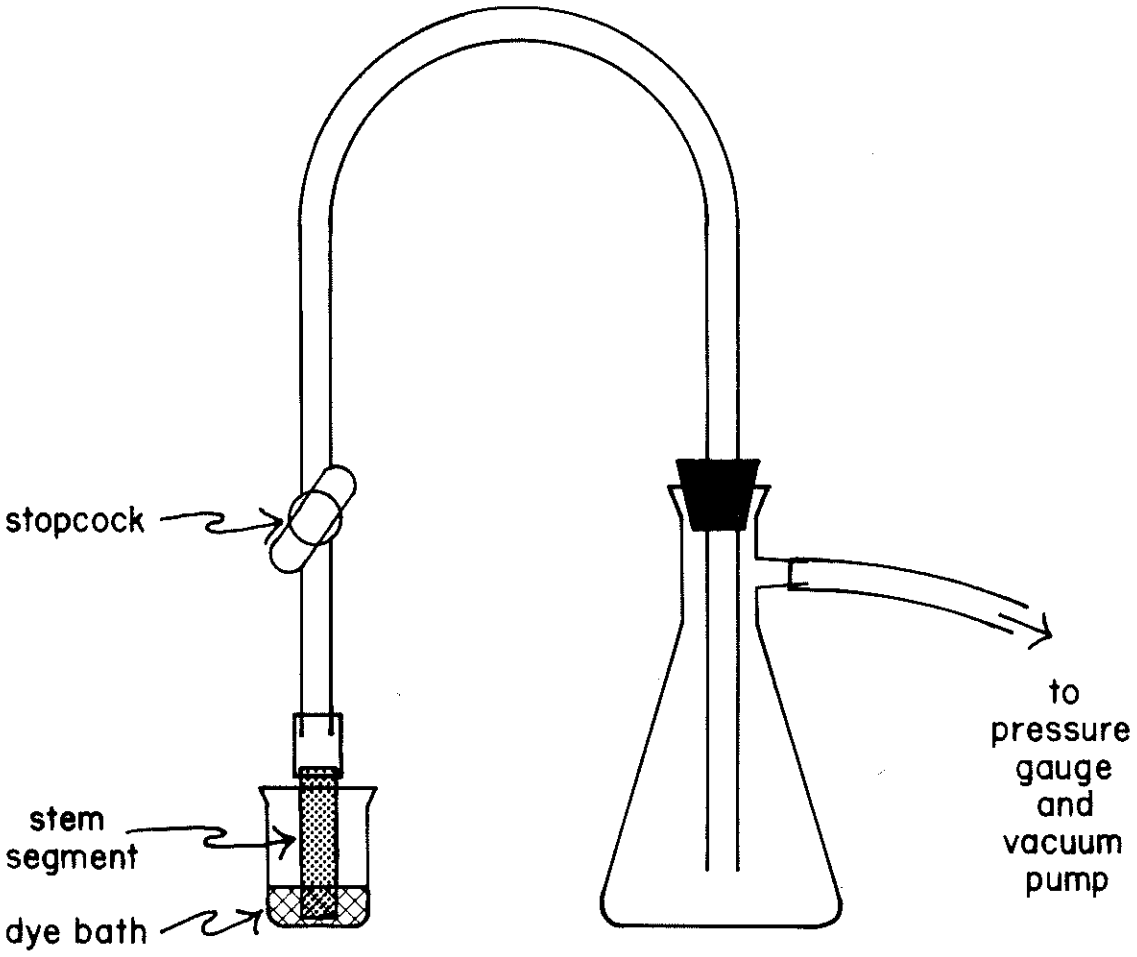
stopcock
stem segment
dye bath
to pressure gauge and vacuum pump

Fig. 4.4. Diameter classes of conducting and non-conducting tracheids of a stem segment dehydrated to 4.0 MPa bomb pressure. Only small diameter tracheids conduct at this bomb pressure.

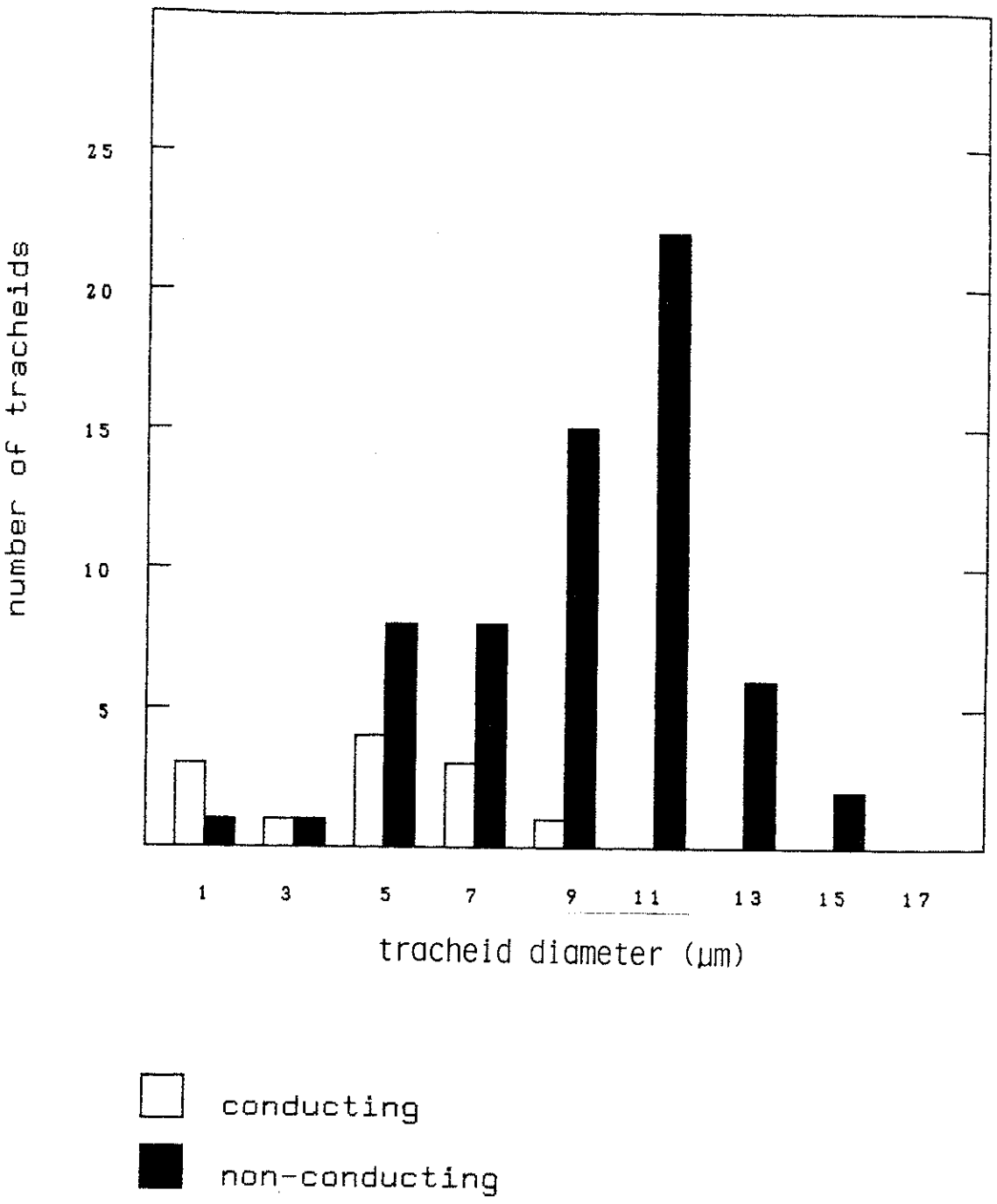
number of tracheids
25
20
15
10
5
1
3
5
7
9
11
13
15
17
tracheid diameter (µm)
conducting
non-conducting

Fig. 4.5. Diameter classes of conducting and non-conducting tracheids in the second growth ring of 4 sements which were dehydrated to various bomb pressures. As tissue is dehydrated to increasing bomb pressures, fewer large diameter tracheids conduct.

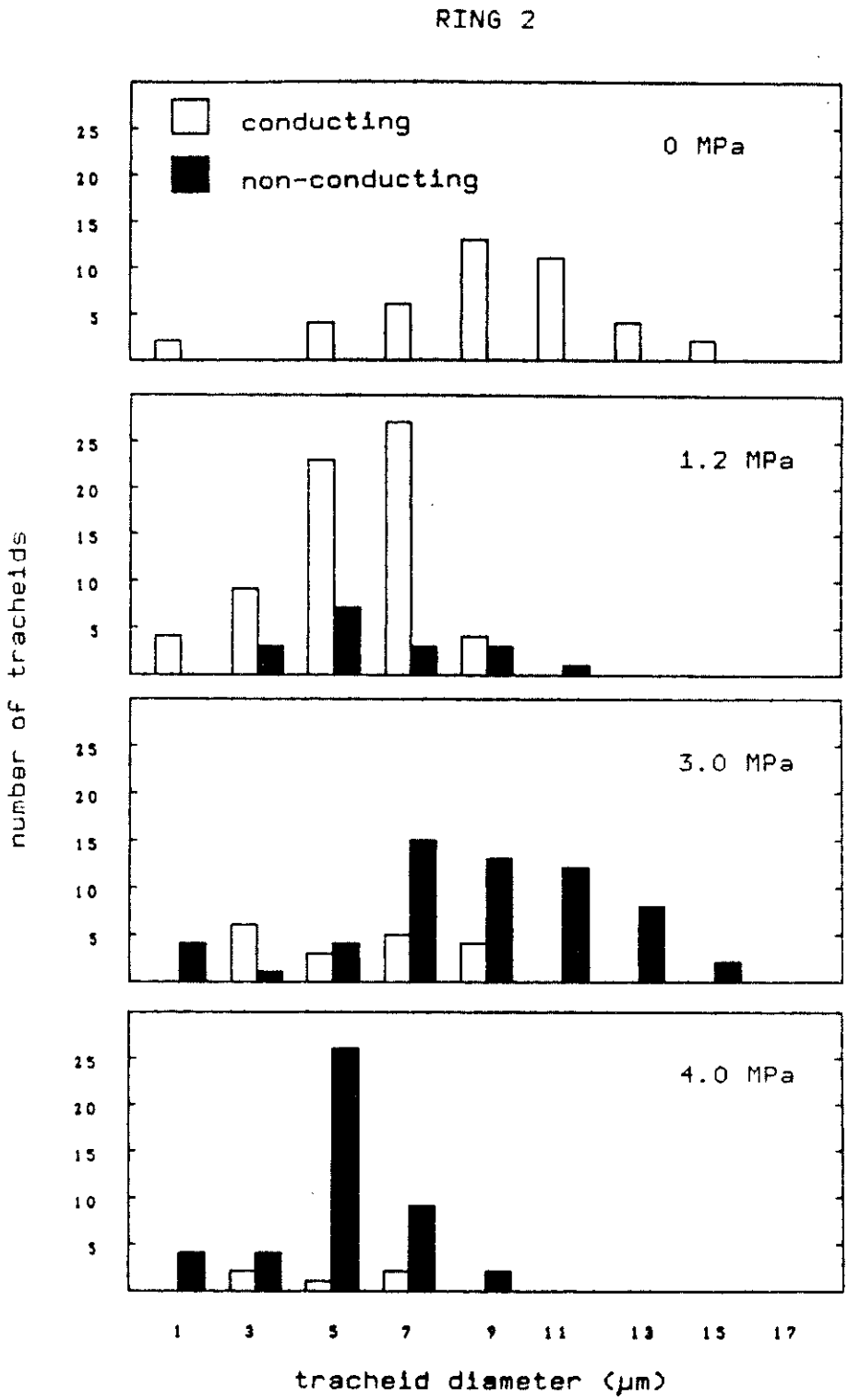
RING 2
conducting
non-conducting
0 MPa
1.2 MPa
3.0 MPa
4.0 MPa
number of tracheids
tracheid diameter (μm)
25
20
15
10
5
1
3
5
7
9
11
13
15
17

Fig. 4.6. Diameter classes of conducting and non-conducting tracheids in growth rings 1 to 4 at a bomb pressure of 1.2 MPa. Tracheids in the inner growth rings begin to embolize before (at lower bomb pressures) the tracheids in the outer growth rings.

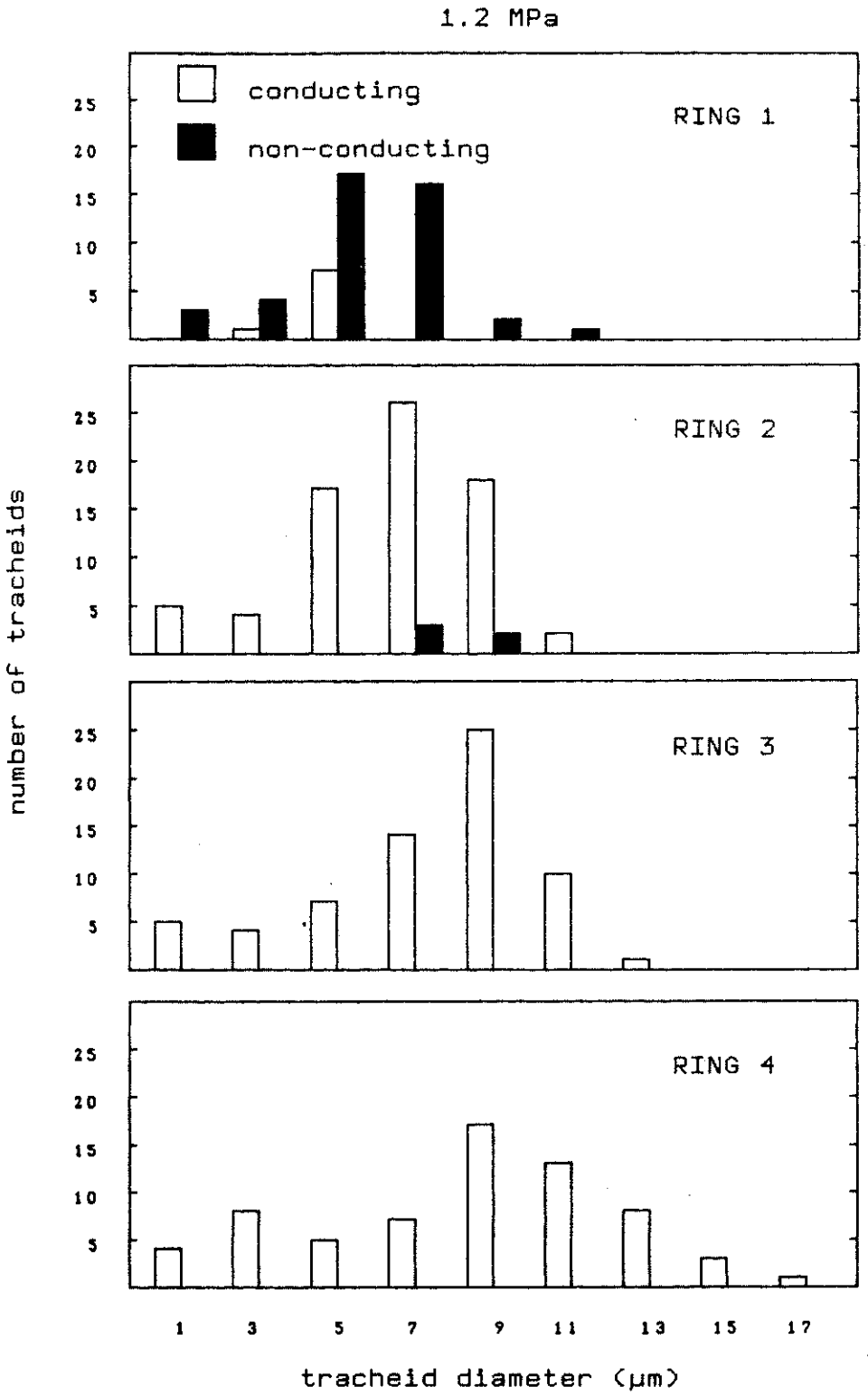
1.2 MPa
conducting
non-conducting
RING 1
RING 2
RING 3
RING 4
number of tracheids
tracheid diameter (µm)
25
20
15
10
5
1
3
5
7
9
11
13
15
17

Fig. 4.7. Relationship between the average diameter of stained (conducting) tracheids and the bomb pressures to which the segments were dehydrated. The average tracheid diameter is expressed as a fraction of the average diameter of all tracheids in the segment. To ease the comparison of graphs produced for pressure bomb dehydrations and for countertop dehydrations (where percent weights are on the abscissa), and to ease the comparison of this data and data reported by other authors using water potential rather than bomb pressure, negative bomb pressure is reported for the X-coordinate in the scatter plots generated from pressure bomb dehydrations. The negative bomb pressure is taken to be the water potential to which each segment was dehydrated.

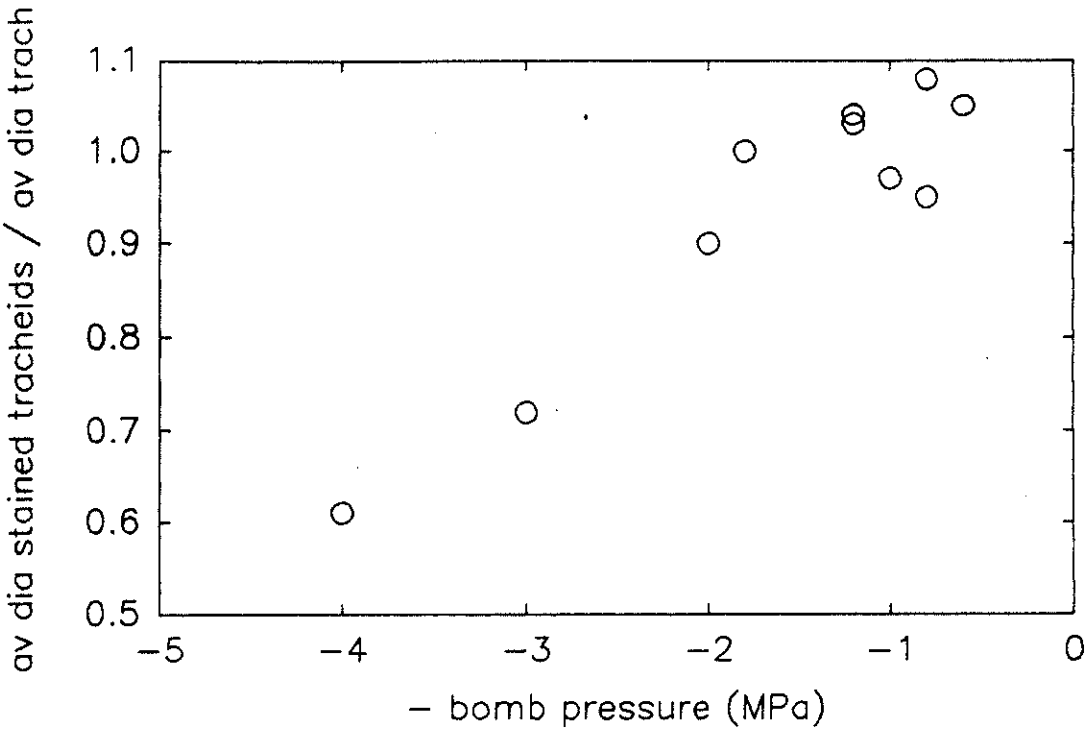
av dia stained tracheids / av dia trach
1.1
1.0
0.9
0.8
0.7
0.6
0.5
−5
−4
−3
−2
−1
0
− bomb pressure (MPa)

Fig. 4.8. Scanning EM of a portion of a *T. occidentalis* pit membrane. Arrows indicate pores in the margo. Scale = 1 μm.

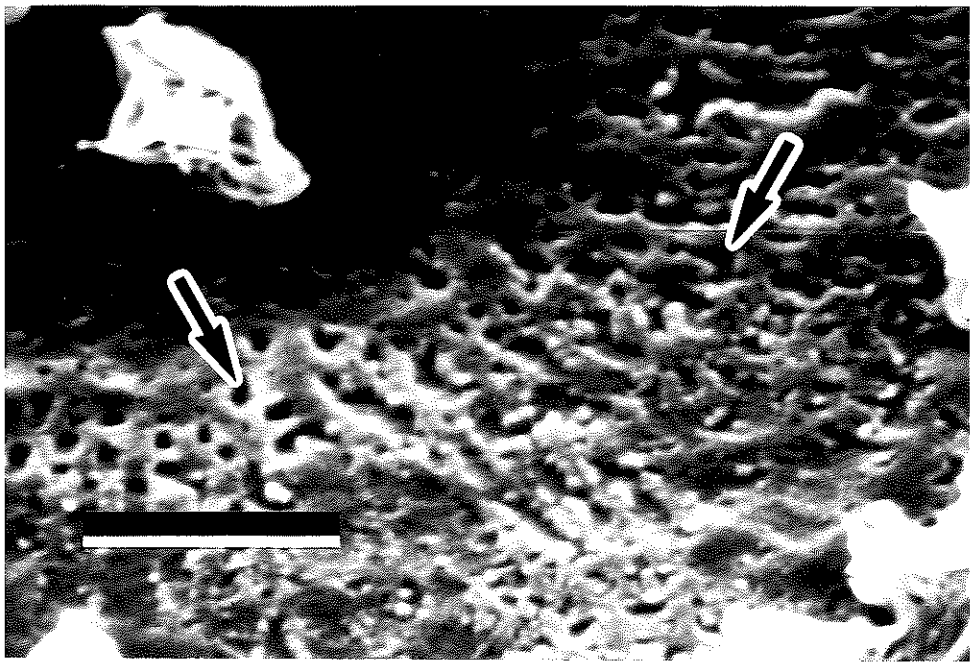

Fig. 4.9. Scanning EMs of particles (arrows) which passed through stem segments of *T. occidentalis* and were collected on chromatography paper. A, Brown iron oxide particles. Scale = 1 μm. B, India ink particles. Scale = 1 μm.

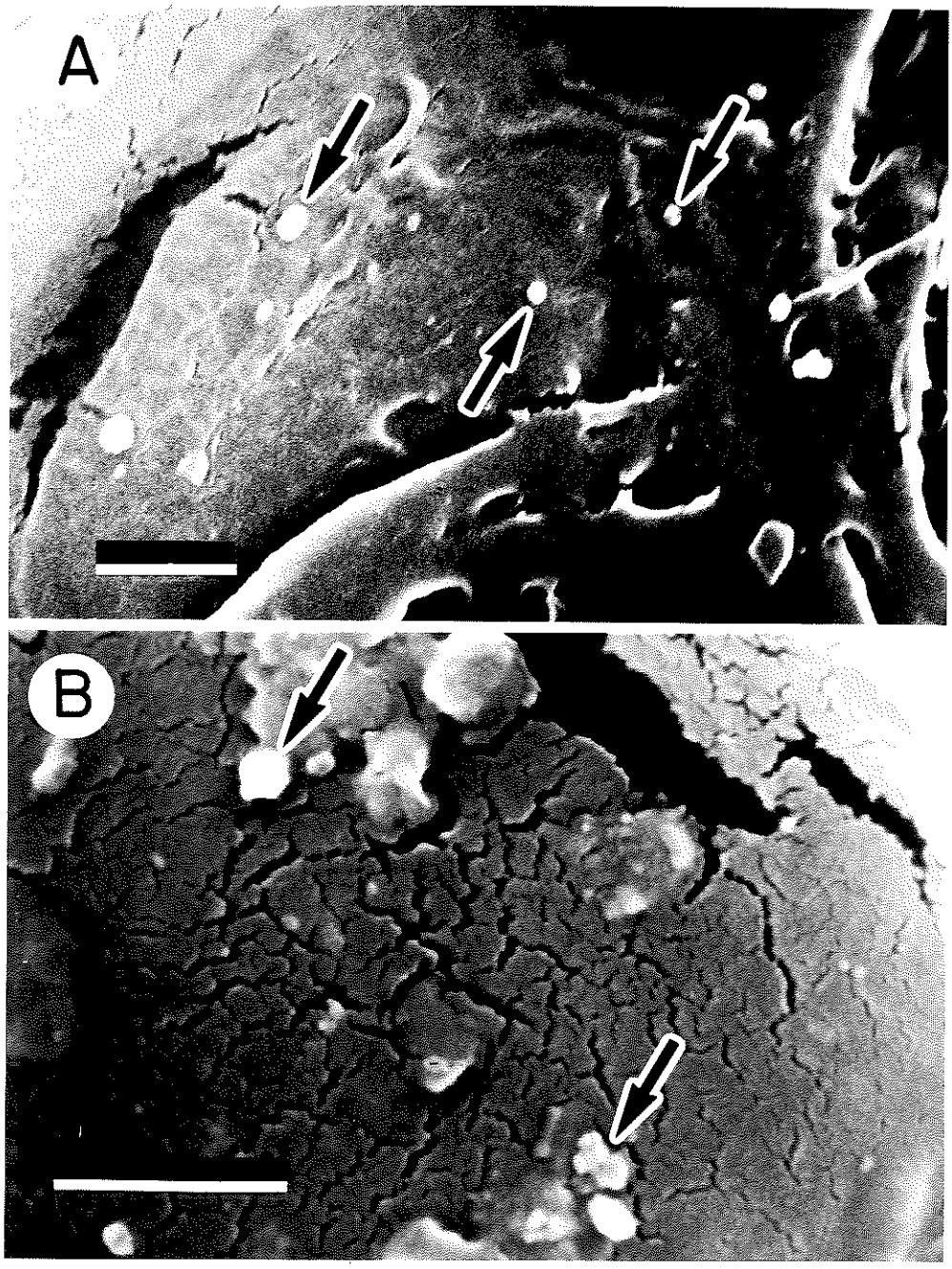
A
B

Fig. 4.10. Scanning EM of monodispersed polystyrene beads which did not pass through the pores of *T. occidentalis* pit membranes. The beads are shown here to have collected in the pit chamber of the tracheid below the plane of the photograph. The view is from the tracheid above the picture plane into the chamber of the adjacent pit. Both the wall of the near tracheid and the pit membrane were removed during sectioning. Very few beads were found in tracheids downstream from the tracheids cut at the surface of application. Scale = 1 μm.

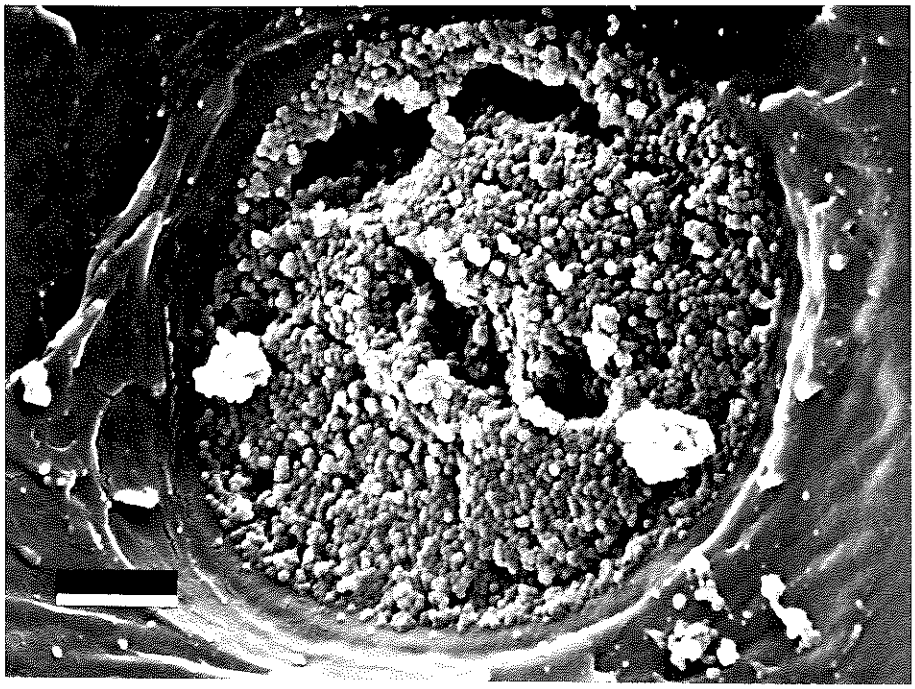

Fig. 4.11. Two curves typical of those used to compare the cumulative weight of water expressed from stem segments in pressure bomb dehydrations with the bomb pressure at which the water was collected. A rapid increase in the weight of expressed water occurs at -1.0 MPa in A and at -1.2 MPa in B. The axes are not at the same scale in A and B. N.B., In this graph and some of the following graphs, negative bomb pressure is used to approximate Ψ_p for each segment at the bomb pressure to which it was dehydrated.

A

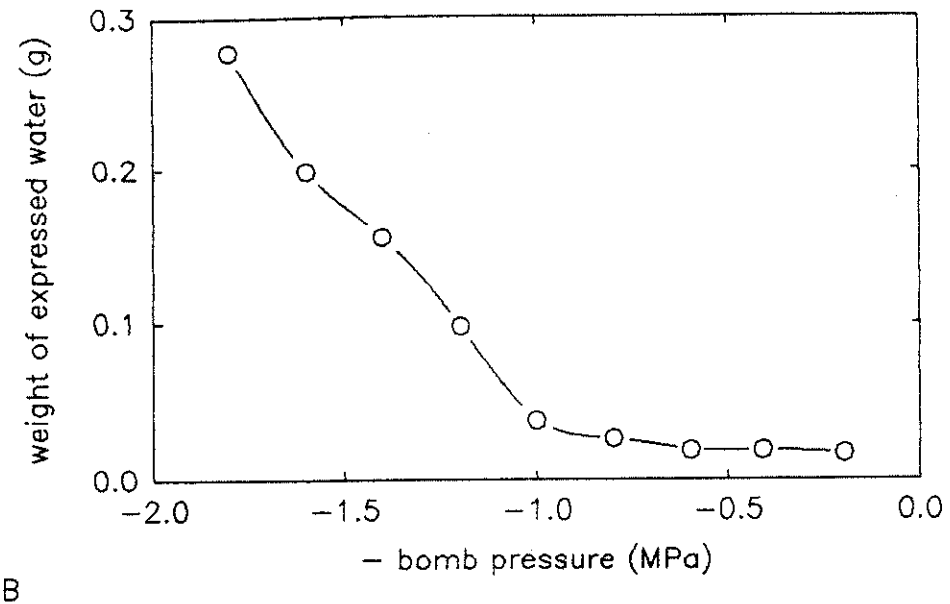
0.3
0.2
0.1
0.0
weight of expressed water (g)
−2.0
−1.5
−1.0
−0.5
0.0
− bomb pressure (MPa)

B

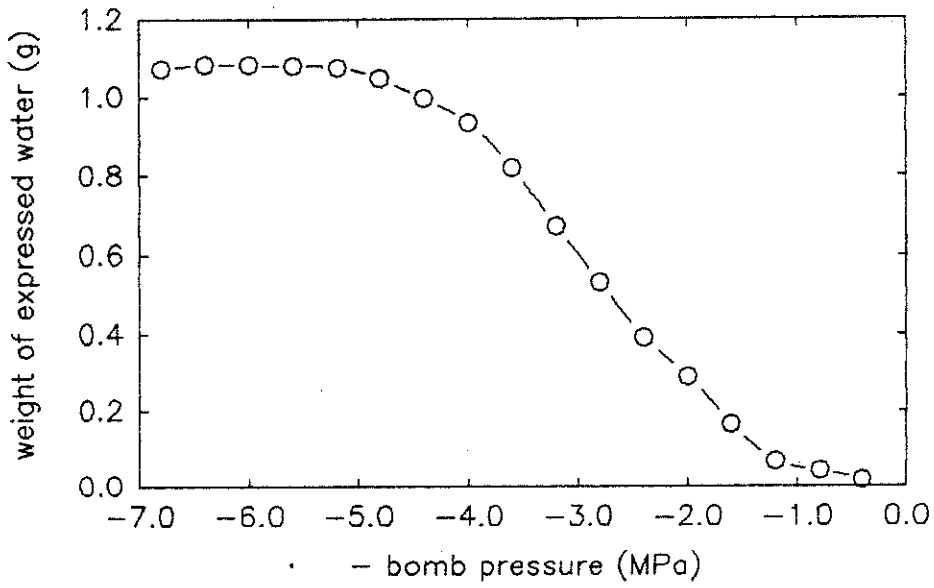
1.2
1.0
0.8
0.6
0.4
0.2
0.0
weight of expressed water (g)
−7.0
−6.0
−5.0
−4.0
−3.0
−2.0
−1.0
0.0
− bomb pressure (MPa)

Fig. 4.12. A, Percentage of tracheids that were stained (conducting) in stem segments which were dehydrated to various bomb pressures. B, Calculated percentage of maximum conductivity in stained (conducting) tracheids of stem segments which were dehydrated to various bomb pressures. Percentage of maximum conductivity was calculated using the equation,

$$\% \text{ conductivity} = 100\ \Sigma(r^4_{\text{stained tracheids}})/\Sigma(r^4_{\text{total}}).$$

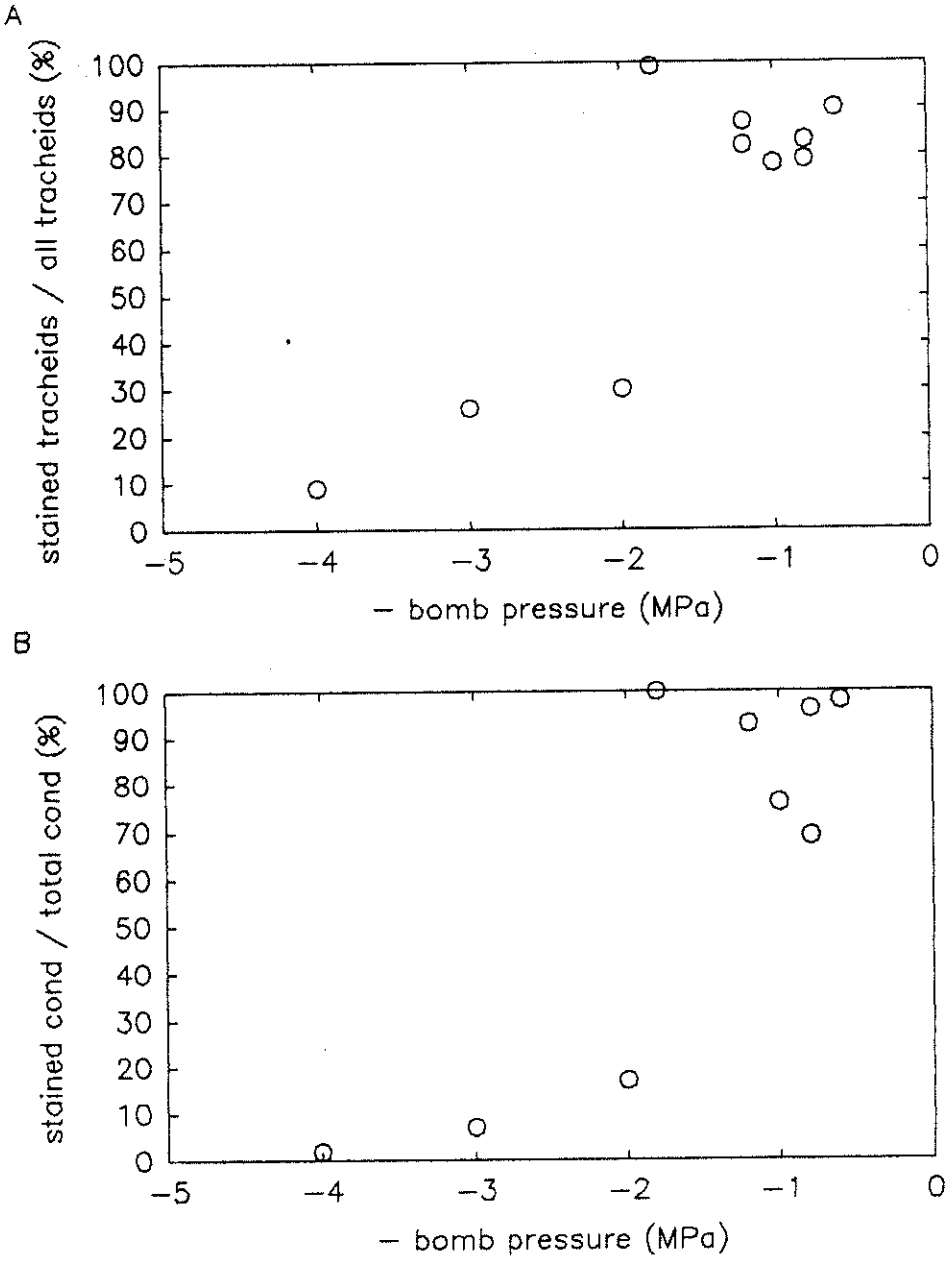
A
stained tracheids / all tracheids (%)
100
90
80
70
60
50
40
30
20
10
0
−5
−4
−3
−2
−1
0
− bomb pressure (MPa)
B
stained cond / total cond (%)
100
90
80
70
60
50
40
30
20
10
0
−5
−4
−3
−2
−1
0
− bomb pressure (MPa)

Fig. 4.13. Percentage of tracheids that stained (conducted dye) after stem segments were dehydrated to various final weights. Final weight is expressed as a percentage of wet (initial) weight. A, Pressure bomb dehydrations. A data point is missing. Estimates indicate that it falls within the encircled area. B, Countertop dehydrations.

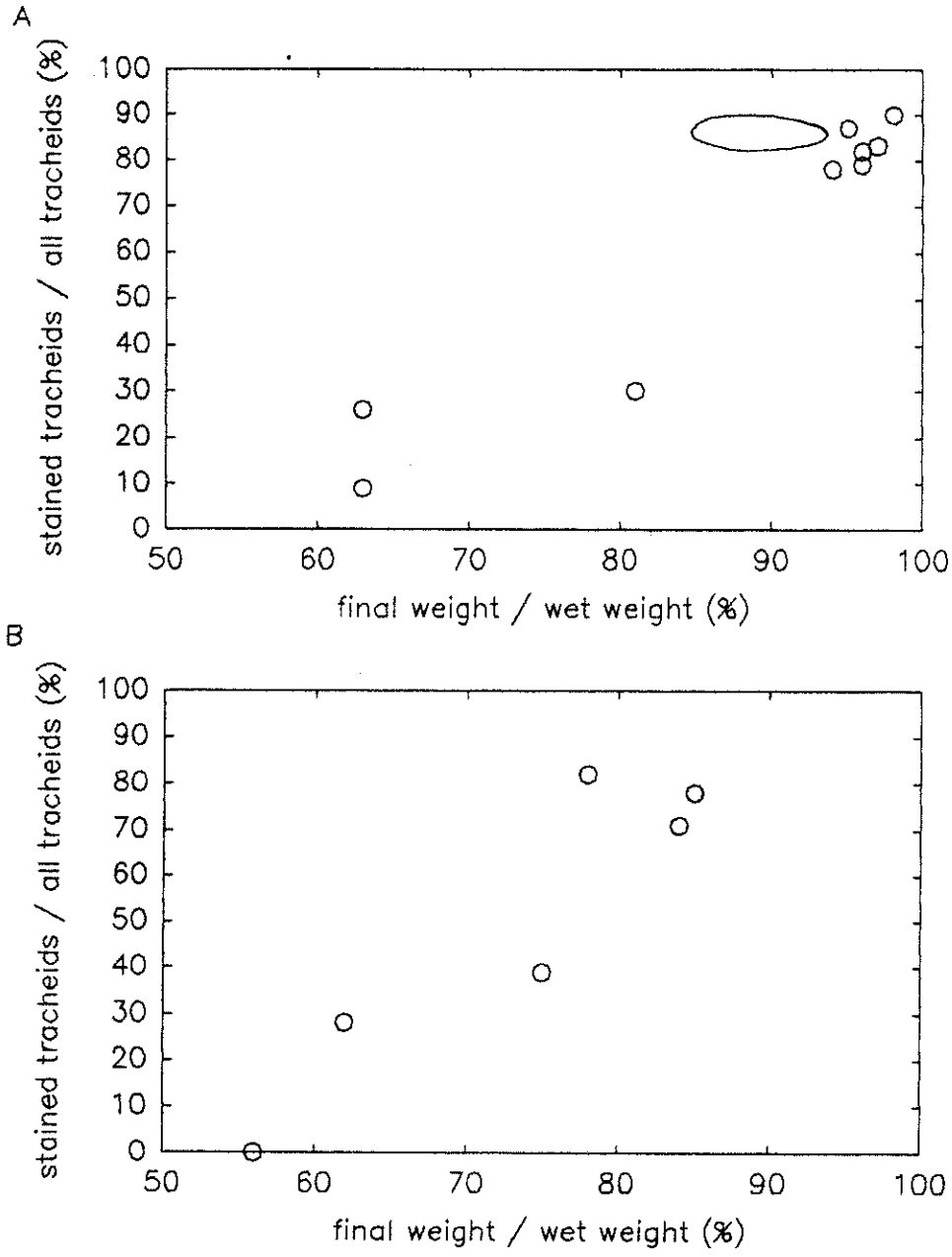
A
stained tracheids / all tracheids (%)
100
90
80
70
60
50
40
30
20
10
0
50
60
70
80
90
100
final weight / wet weight (%)
B
stained tracheids / all tracheids (%)
100
90
80
70
60
50
40
30
20
10
0
50
60
70
80
90
100
final weight / wet weight (%)

Fig. 4.14. Final weight expressed as a percentage of wet (initial) weight of stem segments dehydrated to various bomb pressures.

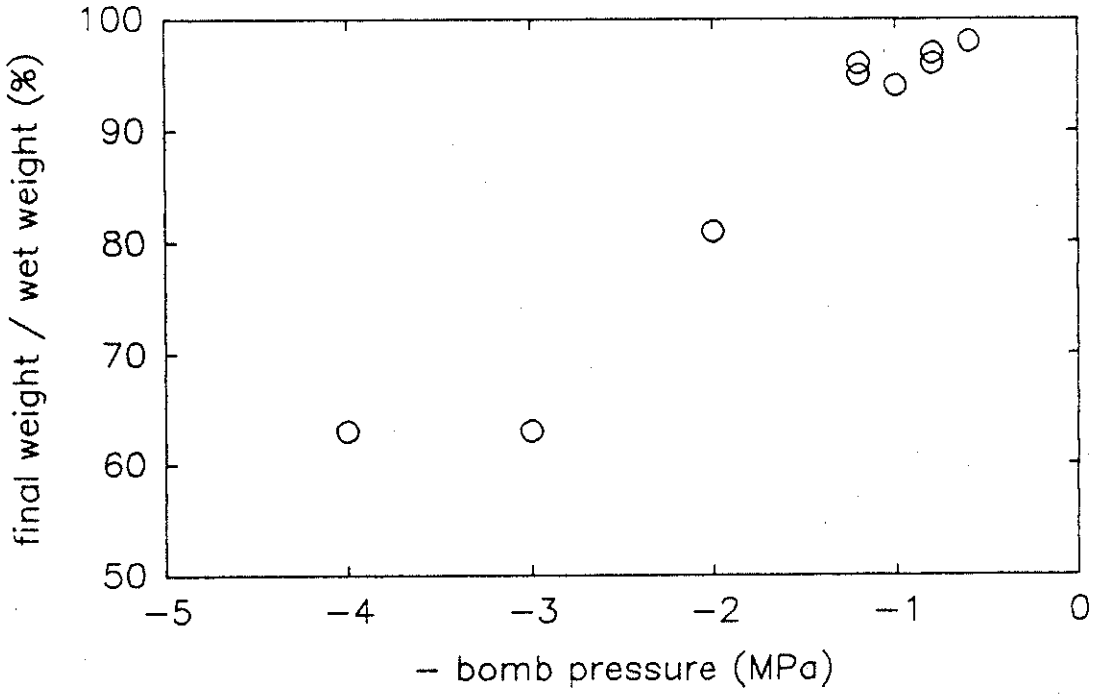
100
90
80
70
60
50
final weight / wet weight (%)
−5
−4
−3
−2
−1
0
− bomb pressure (MPa)

CHAPTER 5

Conclusions

When a sap-filled vessel, tracheid, or fiber in the xylem is subjected to water stress, tension builds in the conduit lumen. The ultrastructure of the cell wall determines the lowest pressure that the lumen can withstand before the integrity of the water column breaks. The limit of tension in undamaged conduits is determined by the diameter of the largest pit membrane pore that is in contact with air in an adjacent lumen. The capillary equation describes the relationship between the pore diameter and the lowest pressure that can be attained in the lumen before the water column breaks. This relationship can be simplified to $\Delta P \tilde{=} 0.3/D$, where ΔP is the pressure difference (MPa) between the conduit lumen and the exterior, or the pressure differential across the meniscus, and D is the diameter (μm) of the largest pore in contact with external air. When the lumen pressure reaches this threshold, external air is pulled into the lumen in the form of a bubble. Some of the lumen water evaporates into the bubble, and some of the water flows to surrounding tissue as the pressure is released. The bubble expands, creating an embolus and blocking the flow of xylem sap through the lumen. Initiation of an embolus by the entry of external air into a cell lumen is known as "air-seeding." If a bubble is trapped in the lumen at the onset of

dehydration, it expands to form an embolus. The debate concerning the variability of the tensile strength of water can now end. The structure of the container and the presence of nucleation sites (e.g., entrapped bubbles) sets the limit on the tension that water in a conduit can withstand before the water column breaks. The physical properties of water itself do not limit lumen tensions.

In both *Sphagnum* hyalocysts (Chap. 2) and *Thuja occidentalis* tracheids (Chap. 3), an individual embolus was observed to form by air-seeding or by expansion of a free-floating entrapped bubble. When a bubble is trapped in a hyalocyst or in a tracheid lumen at the onset of dehydration, the pre-existing bubble expands gradually during dehydration, to form the embolus which blocks sap transport through the lumen. It was not possible in these experiments to recognize a tracheid in which a bubble was present with a diameter smaller than that of the largest pit membrane pores. Bubbles of this diameter are smaller than the limit of resolution of the light microscope. But in hyalocysts, the smaller the bubble diameter, the more rapid is the rate of collapse (diameter reduction). In hyalocysts that have a large reservoir of external water, the lifespan of very small free-floating bubbles is short, so that bubbles with diameters smaller than the pores are unlikely to exist at the onset of dehydration. Air-seeding was not detected in hyalocysts containing bubbles, even when the bubble diameters were much smaller than the smallest diameter hyalocyst pores. If bubble dynamics in *Sphagnum* are indicative, the few very small bubbles that happen to be trapped in tracheids at the onset of dehydration should also expand to fill the tracheid lumens, just as the larger bubbles trapped in tracheids did.

No ultrasonic acoustic emission (AE) is produced when a tracheid with an entrapped bubble dehydrates under tension, but AEs are produced simultaneously with bubble formation in fully hydrated tracheids (Chap. 3). AEs can be used to determine the incidence of cavitation, and thus the incidence of air-seeding which leads to embolism in fully hydrated *T. occidentalis* tracheids. *Sphagnum* hyalocysts do not produce AEs at a volume or frequency that can be consistantly detected with current acoustic equipment (Chap 3). Zimmermann (1983) used the term "air-seeding" to describe the process of water release from *Sphagnum* hyalocysts, so air-seeding, as he defined it, can occur without the production of detectable ultrasonic AEs. Since AEs do not accumulate when a stem segment is dehydrated by the application of positive pressure (Chap. 3), we must conclude that the dynamics of embolism under tension and the dynamics of embolism by positive pressure are different. Because, in general, high energy events produce high frequency signals, such as ultrasonic AEs, it is reasonable to conclude that the process of an air bubble entering a cell under positive pressure is not as energetic an event as entry into a lumen under tension. Unfortunately, too little is known about the production of AEs in xylem to come to definite conclusions. As discussed in Chapter 3, it is important to determine how the structure of conduits and the processes of embolus formation interact to produce the particular characteristics of AEs.

The possibility of embolus formation by other means, such as nucleation at a hydrophobic wall surface, has not been excluded by these experiments. In fact, a gas bubble trapped in a hydrophobic, conical crack could nucleate cavitation at the same tension as a

hydrophilic pore with the same radius opening (Pickard. 1981). Investigation of that mechanism (and any others which have yet to be proposed) for the embolism of xylem conduits should be one of the priorities in water relations research. This research does show that at least two mechanisms, air-seeding and expansion of an entrapped bubble, function in the range of plant water potentials that have been recorded in the field (Chaps. 3 and 4). These water potentials (Ψ = -8.0 to 0.5 MPa) lead to lumen tensions that are far less extreme than those required to break water columns by the spontaneous breaking of the intermolecular bonds in water or the spontaneous resolution of xylem sap into water and a previously dissolved gas.

The process of conduit refilling is important to any plant which must continue to transport xylem sap through conduits that have embolized during the course of a day or a season. It is likely that many plants, including herbs (Milburn, 1979), corn (Tyree et al., 1986), grapes (Sperry et al., 1987), and trees (Sperry, 1985; Zimmermann, 1983) must do this. The dynamics of bubble collapse during refilling are critical to the efficiency of xylem transport after periods of dehydration or winter freezing. Very little is known of the refilling process (see Ewers, 1985; Sperry, 1986; and Sperry et al., 1987 for the most comprehensive studies in this area), yet it is an important area for future research.

In addition to the areas mentioned above, there are several directions in which future embolism research may proceed. A logical extension is to look at the relationship between embolism and the water relations of the whole plant. This thesis gives a glimpse into the complexities of the relationship between xylem anatomy and water

transport. As usual in the sciences, the more we know, the more we realize we don't know. We don't know how xylem ultrastructure varies between species and within species. We don't know how much control genetics and habitat have on ultrastructure. We know little of the relationship between xylem ultrastructure and water relations as it varies within the plant by organ, height, growth ring, or age of the conduit. To date only Bailey (1916) reports a systematic study of woody xylem ultrastructure as it varies with height. Tyree, Sperry, and co-workers are well into projects designed to expand the number of species in which embolism and water relations are studied. Important research by such authors as Milburn and Zimmermann has contributed and will continue to contribute to the body of information on plant water relations. Likewise, the work of Ewers (1985) on winter freezing and embolism, and the work in progress of Ewers and Fisher on the water relations of lianas extends the limits of knowledge and makes possible a more thorough understanding of the interaction of structure and function. Reports by these workers show that water released by embolism of xylem conduits acts as a "safety valve" when plants are under water stress to prevent or delay the dehydration of living tissue to the point of cell death (in particular, see Dixon et al., 1984).

There may be similar processes working to regulate water relations in other circumstances. Hydathodes are structures in which water in tracheids has easy access to the plant exterior through exposed tracheid tips or through the surrounding air space in a matrix of loosely packed, achlorophyllous parenchyma beneath permanently open stomata. In young leaves hydathodes exude water droplets; in older leaves, the hydathodes suberize and cease exudation. The hydathodes

may function not only to prevent flooding of the leaf mesophyll in plants while root pressure is in effect, but they may also direct the nutrient-containing xylem sap towards younger, actively growing leaves when transpiration is low and root pressure is high (Zimmermann, 1983). Under tension, hydathodes may ensure that more mature, photosynthetically active leaves are the last to develop emboli. The hydathodes of more mature leaves are sealed, so that a pathway for embolism, beginning at the exposed hydathode tracheids of young leaves, may exist to ensure that released water is directed to the more axial or basipetal parts of the plant. Under these circumstances, younger leaves with hydathodes give up their water to maintain the hydration of more mature leaves. An interesting example of this may be the mangrove, *Ceriops decandra* which has hydathodes on its petals (Fig. 5.1). This is an unusual feature and may be of real benefit for a plant that grows under conditions which place its roots at very low Ψ in salt water (Sperry, personal communication). When fixed, excised petals of *C. decandra* are dehydrated under the microscope, the emboli develop in the hydathodes and progress basipetally.

The extension of xylem structure and function research into the areas mentioned above is a long-term goal which is being tackled by a small collection of people working independently and in groups. My most immediate plans involve two types of projects. The first group of projects is designed to detail and to clarify the results reported in this thesis. Preliminary work has been completed for each of these projects, and for the most part, only final data collection remains. As previously mentioned, dye ascent experiments on both countertop and pressure bomb dehydrations of *T. occidentalis* will be repeated. A stem

psychrometer will be used to directly measure water potential to reduce error and to ease the comparison of the two dehydration methods. Both SEMicrography and particle infiltration will be used to determine pore diameter of pit membranes. A method for the rapid determination of pore diameter in earlywood and latewood of different growth rings by particle infiltration is in the final stages of development. Similarly, partial data have been collected to quantitatively correlate length of dehydration and length of rehydration with the presence of entrapped bubbles. A method to compare the number of AEs detected upon dehydration with the exact number of intact tracheids in a wood sample is almost complete. The shuttle microscope/movie film method of Zimmermann and Tomlinson (1966) should make possible the determination of the exact number of intact tracheids in a very small wood sample.

The second group is intended to broaden our understanding of embolism in other species and, at the same time to increase our understanding of dehydration dynamics. Among these projects are repetitions of the AE/dye ascent/embolus initiation experiments on *Thuja plicata* (pit membrane structure differs from that of *T. occidentalis*) and *Pinus strobus* (pit membrane structure differs from that of *Thuja*, and AE characteristics and water potential at embolism are known to differ from from those of *T. occidentalis* and *Acer saccharum*). The results of these experiments, in conjunction with similar experiments conducted by other workers on angiosperms and with the work by Tyree on AE characteristics should greatly improve the understanding of the relationship between xylem anatomy and AE production and characteristics.

Concurrently, I plan to work on the dynamics of bubble collapse in

water conduits because the ability to refill is intimately tied to a tracheary element's susceptibility to embolism and is critical to xylem function.

LITERATURE CITED

Bailey IW 1916 The structure of the bordered pits of conifers and its bearing upon the tension hypothesis of the ascent of sap. Bot Gaz 62: 133-142, 1 plate

Dixon MA, J Grace, MT Tyree 1984 Concurrent measurements of stem density, leaf and stem water potential, stomatal conductance, and cavitation on a sapling of *Thuja occidentalis* L. Plant Cell Environ 7: 615-618

Milburn JA 1979 Water Flow in Plants. Longman, London, New York

Pickard WF 1981 The ascent of sap in plants. Prog Biophys molec Biol 37: 181-229

Sperry JS 1985 Xylem embolism in the palm *Rhapis excelsa*. IAWA Bull ns6: 283-292

Sperry JS 1986 Relationship of xylem embolism to xylem pressure potential, stomatal closure, and shoot morphology in the palm *Rhapis excelsa*. Plant Physiol 80: 110-116

Sperry JS, NM Holbrook, MH Zimmermann, MT Tyree 1987 Spring filling of xylem vessels in wild grapevine. Plant Physiol 83: 414-417

Tyree MT, EL Fiscus, SD Wullschleger, MA Dixon 1986 Detection of xylem cavitation in corn under field conditions. Plant Physiol 82: 597-599

Zimmermann MH 1983 Xylem Structure and the Ascent of Sap. Springer-Verlag, Berlin, Heidelberg, New York, Tokyo

Zimmermann MH, PB Tomlinson 1966 Analysis of complex vascular systems in plants: optical shuttle method. Science 152: 72-73

Fig. 5.1. Photomicrograph of the hairs on a petal of the mangrove *Ceriops decandra*. Inset, Enlargement of the tip of a hair showing the hydathodes, swollen tracheids ends exposed to the plant's exterior.

EPILOGUE

Many of the questions in plant biology pertain to structure/function relationships, at least in part: How do particular cellular organelles function? How do infections, such as *Ceratocystis ulmi* (Dutch elm disease) or *Erwinia amylovora* (rosaceous fireblight), invade and kill or limit the growth of plants? How are certain plant/microbe or plant/animal symbioses beneficial, and how do they function? What limits the growth rates and final dimensions of crop plants and forest trees? To gain a full understanding of the answers to these questions requires an expertise in areas (e.g., chemistry, physics, and engineering) that whole plant biologists have not had in the last half-century. The scientists who work on problems in plants and who are the most likely to have a detailed understanding of the requisite fields, the plant physiologists, and cellular and molecular biologists, rarely relate their work to the biology of the whole plant. The blame for this unfortunate set of circumstances probably lies only in the fact that as understanding grows, more information must be digested within a single field. It is no longer possible for a single person to have an indepth knowledge of fields closely related to his own and to have a solid general background as well. In order to compete in research today, a scientist must usually focus his efforts in one area of research. Rarely can one find a plant physiologist, competent in chemistry, physics, and mathematics, who leads his field in research and who also has solid exposure to systematics, anatomy and

morphology, and ecology, not to mention being able to apply advances in medicine, aerospace technology, and other fields to his research. Unfortunately, as specialization increases, researchers from diverse fields talk with each other less and less.

To make basic research advances that may have applications which can quickly be implemented, requires that people working in different fields collaborate closely. The establishment of multi-disciplinary research groups and centers is being attempted in several areas, especially in engineering, physics, and medicine, to facilitate the exchange of information and expertise (cf., Walsh, 1987). It is time to develop multi-disciplinary groups in the plant sciences. One productive theme for such a group is plant biomechanics, a field that has been neglected for too long and which promises to shed light on many problems that have puzzled plant scientists for many years. As exemplified in this thesis research, many structure/function problems can be answered if attacked from this angle. Discovery of processes specific to plants may also have applications in fields outside of botany and biology. For example, the design of systems based on xylem chemistry and ultrastructure that can withstand pressures at or below vacuum without failing may have important applications in fluids engineering (boat propellers) and in space engineering. A small group of scientists which includes a physiologist, an anatomist/morphologist, an ecologist, and a physicist or an engineer promises to make unparalleled advances in the plant sciences which could lead to important crop and/or forestry applications. The prospect of better information dissemination bodes well for future technological advances. Yet, it is essential that the use of modern technology in research not

displace more traditional methods, including pure observation and description.

It is dismaying to realize that we still struggle with questions from 70 years ago. With the clever use of simple methods, botanists of that time reached answers on which we could not elaborate until recently. When I began this project, there were no laboratories equipped to tackle plant embolism research with the necessary complement of both conventional and modern equipment. We now have the means to reach definitive answers for some of the early botanical questions. Let us take advantage of the wealth of expertise and techniques to put to rest older questions and move on to answer the myriad of others that surface in our pursuit. I hope that this thesis demonstrates the importance of balance in research techniques; neither traditional nor technological methods alone can answer challenging questions in the plant sciences, nor can traditionally trained botanists take these questions to task; we need to enlist the help of people educated as engineers, such as Pickard and Tyree.

LITERATURE CITED

Walsh J 1987 NSF puts big stake on research centers. Science 236: 18-19

LITERATURE CITED (COMPLETE)

Apfel RE 1972 The tensile strength of liquids. Sci Amer 227: 58-71

Bailey IW 1916 The structure of the bordered pits of conifers and its bearing upon the tension hypothesis of the ascent of sap in plants. Bot Gaz 62: 133-142, 1 plate

Bauch J, W Liese, R Schultze 1972 The morphological variability of the bordered pit membranes in gymnosperms. Wood Sci Technol 6: 165-184

Bonner LD, RJ Thomas 1972 The ultrastructure of intercellular passageways in vessels of yellow poplar (*Liriodendron tulipifera*, L.), part I: vessel pitting. Wood Sci Technol 6: 196-203

Carpita NC 1982 Limiting diameters of pores and the surface structure of plant cell walls. Science 218: 813-814

Clymo RS, PM Hayward 1982 The ecology of *Sphagnum*. *In* AJE Smith, ed, Bryophyte Ecology. Chapman and Hall, London, New York, pp 229-289

Cosgrove DJ 1985 Cell wall yield properties of growing tissue: evaluation by *in vivo* stress relaxation. Plant Physiol 78: 347-356

Crombie DS, MF Hipkins, JA Milburn 1985a Gas penetration of pit membranes in the xylem of *Rhododendron* as the cause of acoustically detectable sap cavitation. Aust J Plant Physiol 12: 445-453

Crombie DS, JA Milburn, MF Hipkins 1985b Maximum sustainable xylem sap tensions in *Rhododendron* and other species. Planta 163: 27-33

Dixon HH 1924 The Transpiration Stream. University of London Press, Ltd., London

Dixon MA, J Grace, MT Tyree 1984 Concurrent measurements of stem density, leaf and stem water potential, stomatal conductance and cavitation on a sapling of *Thuja occidentalis* L. Plant Cell and Environ 7: 615-618

Eicke R 1958 Die Bedeutung der Feinstruktur der Hoftüpfel für die Phylogenie der Gymnospermen. Z Botanik 46: 5-15

Eves H 1974 Geometry: mensuration formulas. *In* WH Beyer, ed, CRC Standard Mathematical Tables, Ed. 27. CRC Press Inc, Boca Raton FL, p 124

Ewers F 1985 Xylem structure and water conduction in conifer trees, dicot trees, and lianas. IAWA Bull ns6: 309-317

Huber B 1956 Die Gafässleitung. *In* O Stocker, ed, Encyclopedia of Plant Physiology. Springer, Berlin, Göttingen, Heidelberg, pp 541-582

Hüsken D, E Steudle, U Zimmermann 1978 Pressure probe technique for measuring water relations of cells of higher plants. Plant Physiol 61: 158-163

Li W-H, S-H Lam 1964 Principles of Fluid Mechanics. Addison-Wesley Publishing Co, Reading MA, Menlo Park CA, London, Amsterdam, Don Mills ONT, Sydney, p 276

Liese W, J Bauch 1964 Über die Wegsamkeit der Hoftüpfel von Coniferen. Naturwissenschaften 21: 516

Meylan BA, BG Butterfield 1982 Pit membrane structure in the vessel-less woods of *Pseudowintera dandy* (Winteraceae). IAWA Bull ns3: 167-175

Milburn JA 1973 Cavitation in *Ricinus* by acoustic detection: induction in excised leaves by various factors. Planta 110: 253-265

Milburn JA 1979 Water Flow in Plants. Longman, London, New York

Milburn JA, RPC Johnson 1966 The conduction of sap: II, Detection of vibrations produced by sap cavitation in *Ricinus* xylem. Planta 69: 43-52

Nonami H, JS Boyer, E Steudle 1987 Pressure probe and isopiestic psychrometer measure similar turgor. Plant Physiol 83: 592-595

Oertli JJ 1971 The stability of water under tension in the xylem. Z Pflanzenphysiol 65: S195-209

Pickard WF 1981 The ascent of sap in plants. Prog Biophys molec Biol 37: 181-229

Renner O 1915 Theoretisches und Experimentelles zür Kohäsionstheorie der Wasserbewegung. Jahr wiss Botanik 56: 617-667

Renner O 1925 Die Porenweite der Zellhäute in ihrer Beziehung zum Saftsteigen. Ber dtsch bot Ges 43: 207-211

Scholander PF, HT Hammel, ED Bradstreet, EA Hemmingsen 1965 Sap pressure in vascular plants: negative hydrostatic pressure can be measured in plants. Science 148: 339-346

Siau JF 1984 Transport Processes in Wood. Springer-Verlag, Berlin, Heidelberg, New York, Tokyo

Sperry JS 1985 Xylem embolism in the palm *Rhapis excelsa*. IAWA Bull ns6: 283-292

Sperry JS 1986 Relationship of xylem embolism to xylem pressure potential, stomatal closure, and shoot morphology in the palm *Rhapis excelsa*. Plant Physiol 80: 110-116

Sperry JS, NM Holbrook, MH Zimmermann, MT Tyree 1987 Spring filling of xylem vessels in wild grapevine. Plant Physiol 83: 414-417

Tyree MT, MA Dixon 1983 Cavitation events in *Thuja occidentalis* L.?:

ultrasonic acoustic emissions from the sapwood can be measured. Plant Physiol 72: 1094-1099

Tyree MT, MA Dixon 1986 Water stress induced cavitation and embolism in some woody plants. Physiol Plant 66: 397-405

Tyree MT, MA Dixon, RG Thompson 1984a Ultrasonic acoustic emissions from the sapwood of *Thuja occidentalis* measured inside a pressure bomb. Plant Physiol 74: 1046-1049

Tyree MT, MA Dixon, EL Tyree, R Johnson 1984b Ultrasonic acoustic emissions from the sapwood of cedar and hemlock: an examination of three hypotheses regarding cavitations. Plant Physiol 75: 988-992

Tyree MT, EL Fiscus, SD Wullschleger, MA Dixon 1986 Detection of xylem cavitation in corn under field conditions. Plant Physiol 82: 597-599

Van Alfen NK, BD McMillan, V Turner, WM Hess 1983 Role of pit membranes in macromolecule-induced wilt of plants. Plant Physiol 73: 1020-1023

Walsh J 1987 NSF puts big stake on research centers. Science 236: 18-19

Ward CA, P Tikuisis, RD Venter 1982 Stability of bubbles in a closed volume of liquid-gas solution. J Appl Phys 53: 6076-6084

Weast RC, ed 1968 CRC Handbook of Chemistry and Physics. The Chemical Rubber Co., Cleveland OH

Zimmermann MH 1983 Xylem Structure and the Ascent of Sap. Springer-Verlag, Berlin, Heidelberg, New York, Tokyo

Zimmermann MH, PB Tomlinson 1966 Analysis of complex vascular systems in plants: optical shuttle method. Science 152: 72-73